東京都市大学
TOKYO CITY UNIVERSITY

Status and perspectives of KAGRA

Hirotaka Takahashi
on behalf of KAGRA collaboration

**Research Center for Space Science, Advanced Research Laboratories,
and Department of Design and Data Science,
Tokyo City University, Japan**

KAGRA

hirotaka@tcu.ac.jp

Group HP (English)
https://www.comm.tcu.ac.jp/gw-ds/home-en/

Gravitational Waves

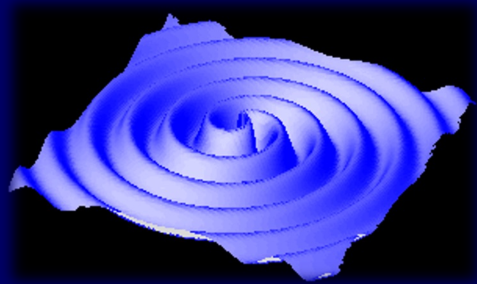

- Transverse waves with
  2 polarizations in General Relativity:

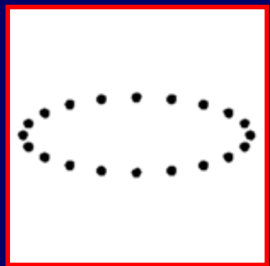

+ polarization

x polarization

- Interferometer measures:
  dL=x-y

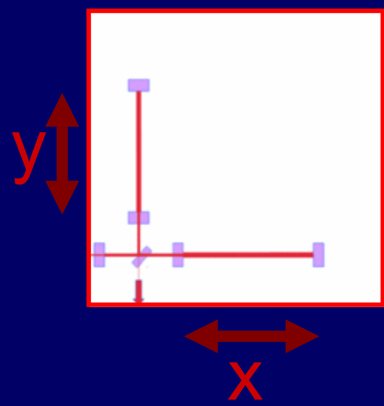

Use a Laser Interferometer to detect GWs

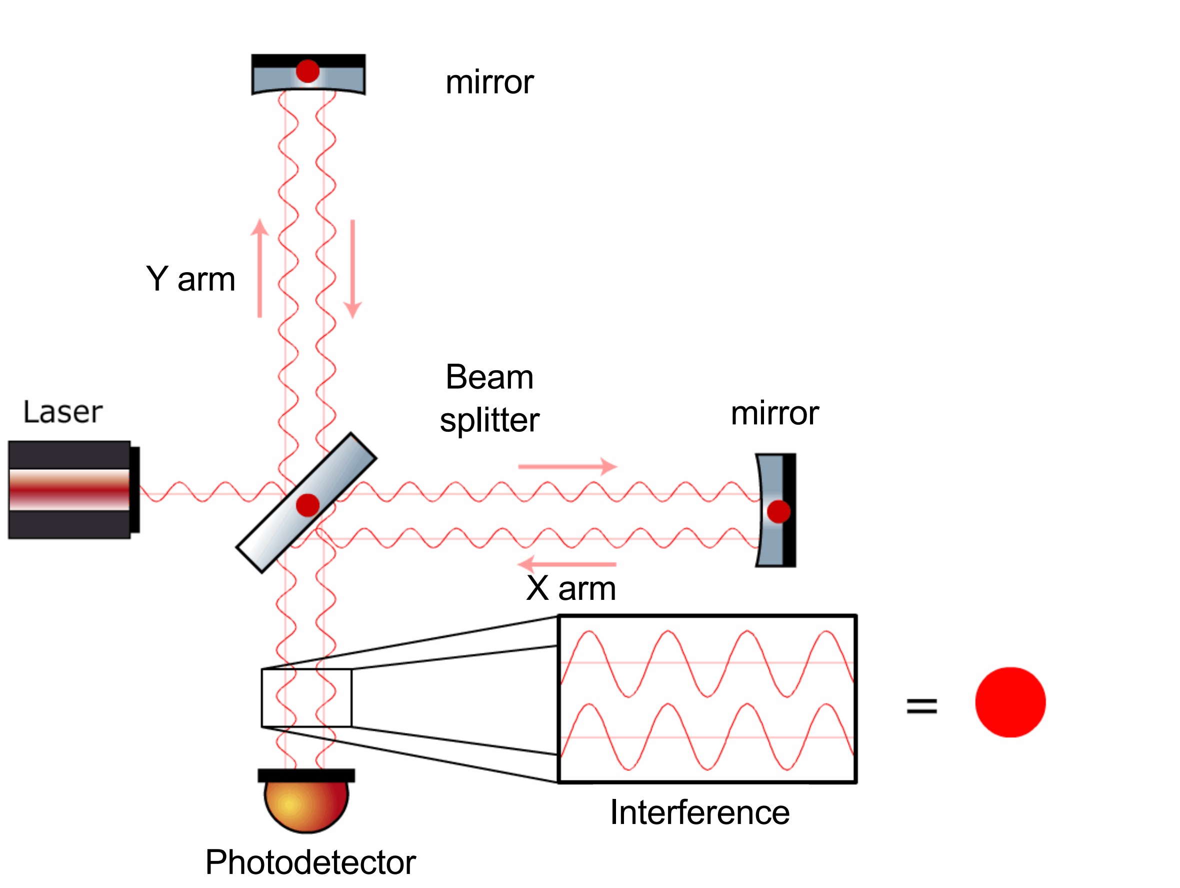

Gravitational-Wave Observatories

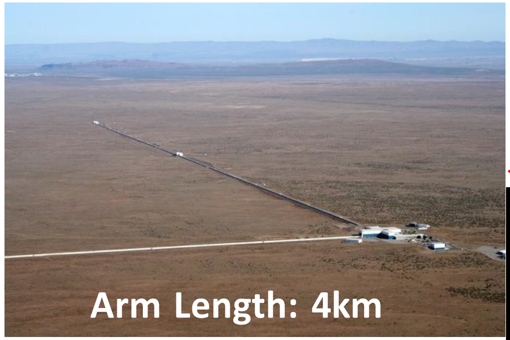

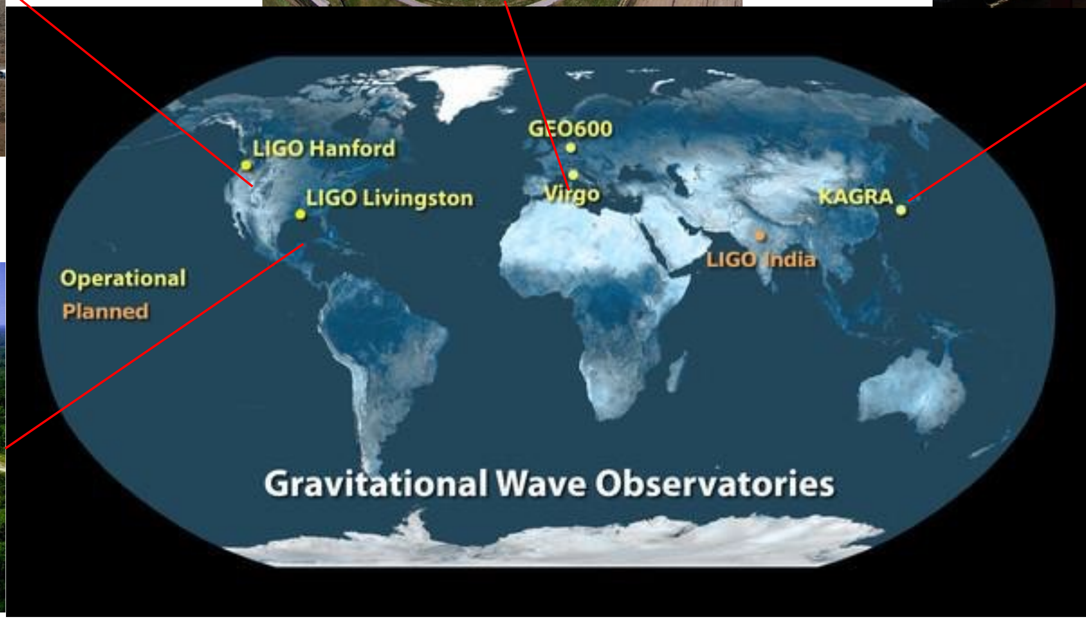

LIGO-Virgo-KAGRA (LVK) collaboration

Figure credit:
Caltech/MIT/LIGO Lab/ICRR

KAGRA

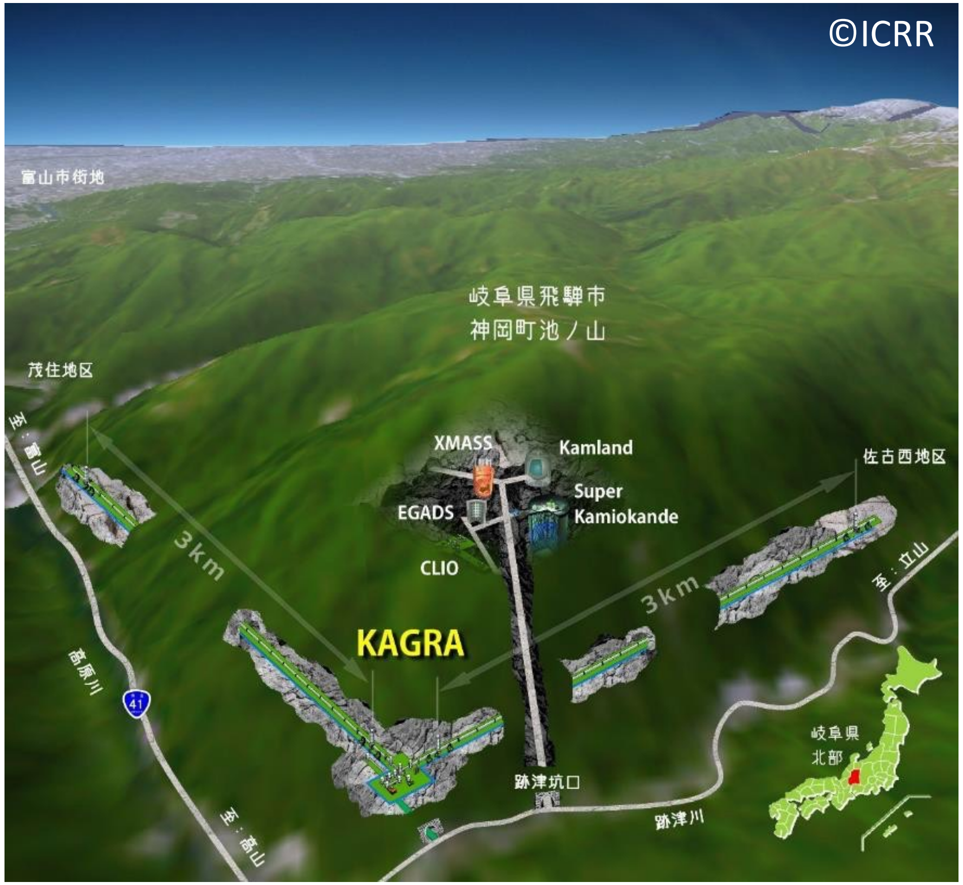

- **Interferometric gravitational-wave (GW) detector** built inside the Kamioka mine in Hida City, Gifu Prefecture, Japan

- Key differences from LIGO/Virgo

  (1) Underground ➔ Improved stability thanks to low seismic noise

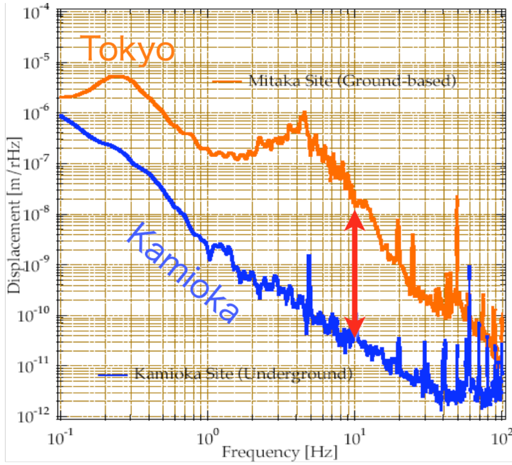

Amplitude of seismic motion

✓ Underground to reduce seismic noises

KAGRA

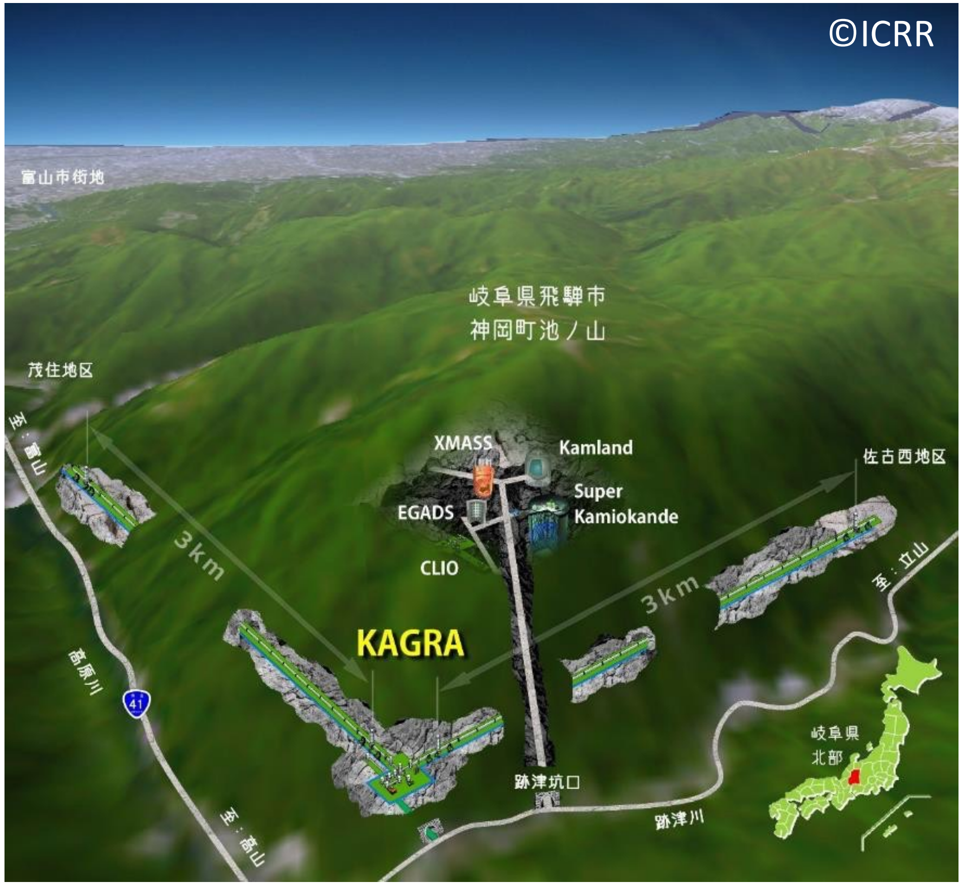

- **Interferometric gravitational-wave (GW) detector** built inside the Kamioka mine in Hida City, Gifu Prefecture.
- Key differences from LIGO/Virgo
  - **(1) Underground ➔ Improved stability thanks to low seismic noise**
  - **(2) Cryogenic mirrors and suspensions ➔ Reduced thermal noise**


KAGRA's cryostat

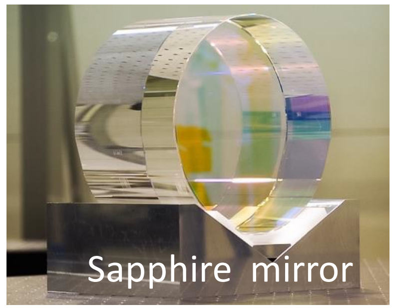
Sapphire mirror

ET Both of these new features are planned to be adopted in a third-generation telescope.

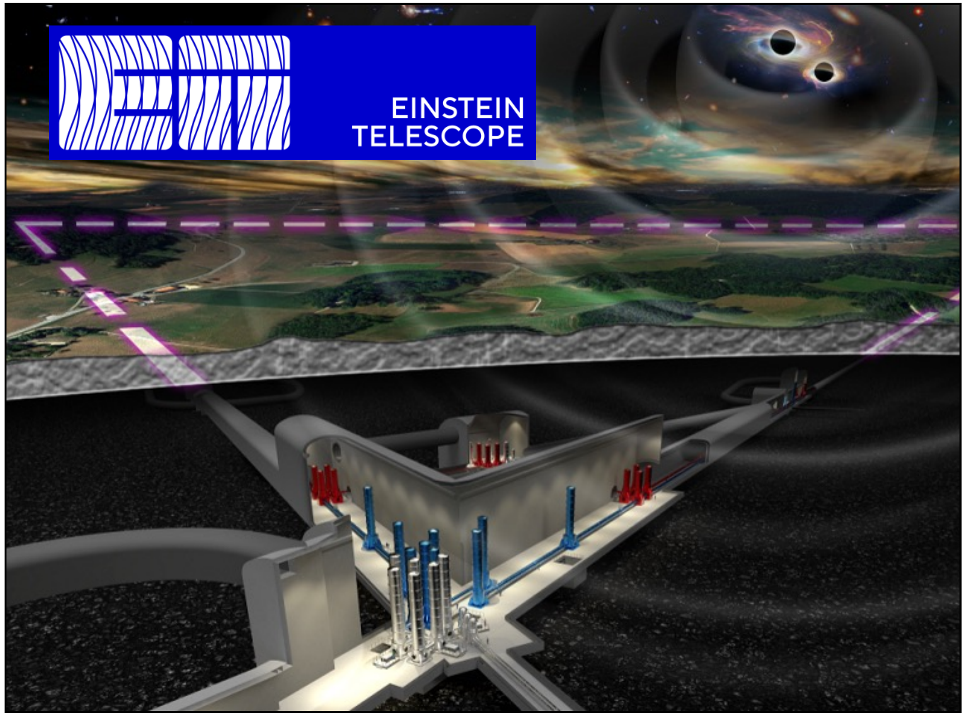

Cryogenic to reduce thermal noises (T=10K @mirrors)

Underground to reduce seismic noises

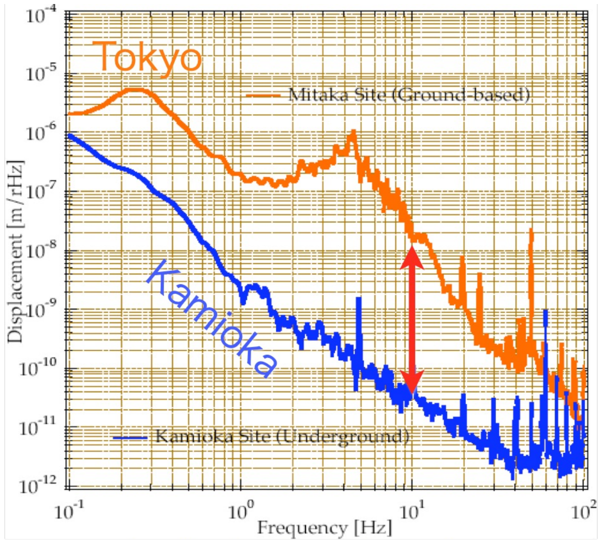

Amplitude of seismic motion

We are on the right track of the progress of science.

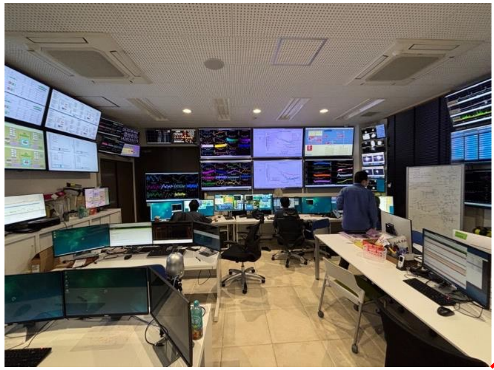

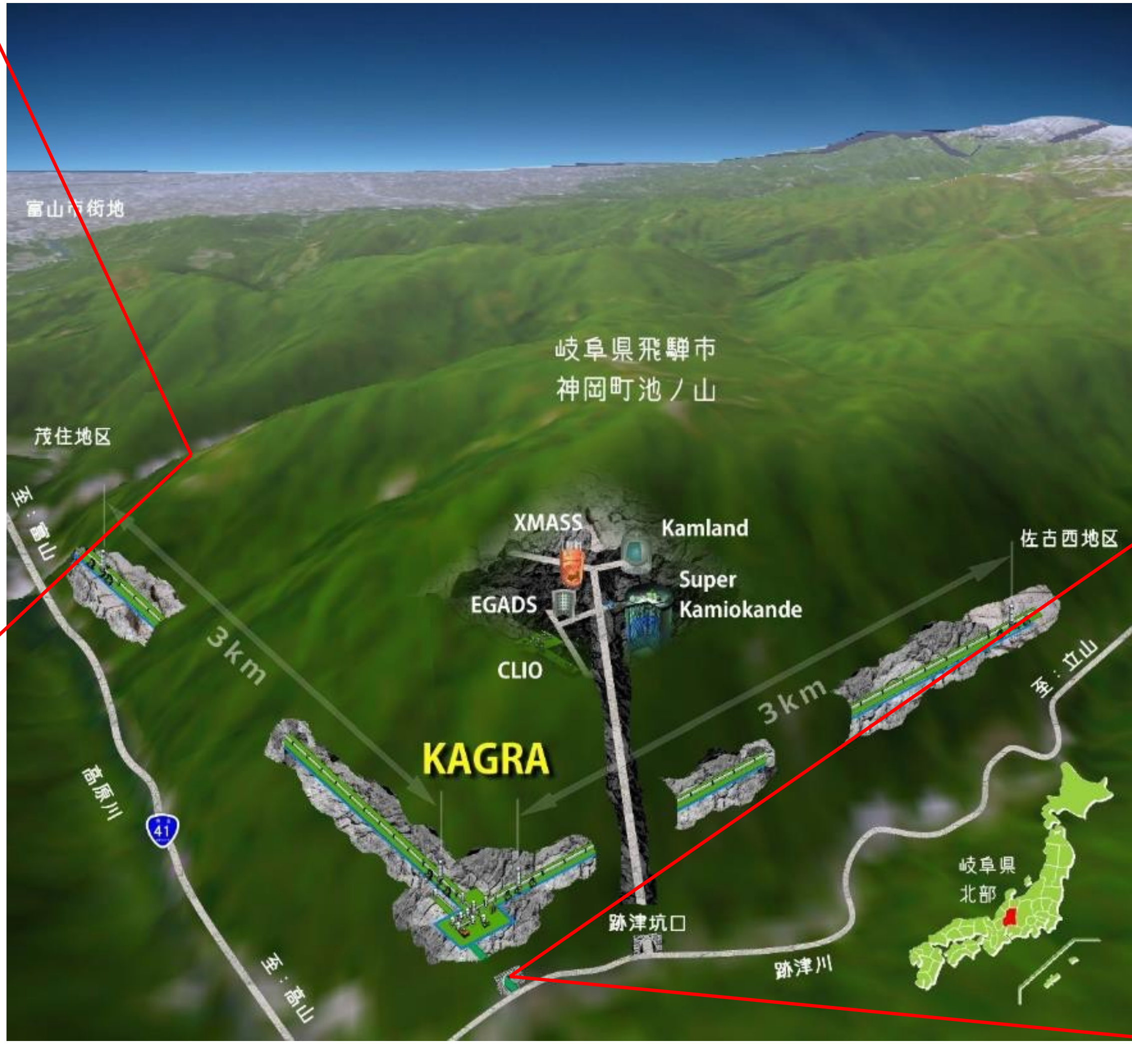
富山市街地
岐阜県飛騨市
神岡町池ノ山
茂住地区
至：富山
XMASS
Kamland
Super
Kamiokande
EGADS
CLIO
3km
3km
佐古西地区
至：立山
KAGRA
高原川
41
跡津坑口
跡津川
岐阜県
北部
至：高山

KAGRA

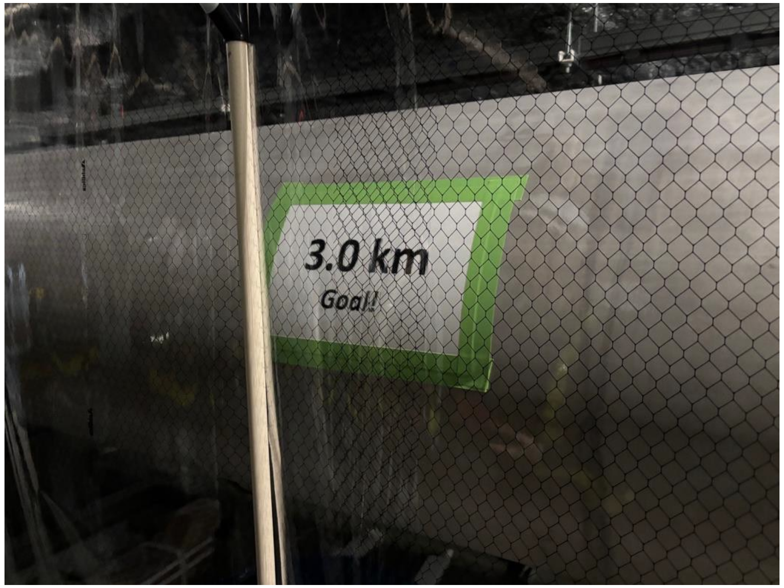

3km arm length, d80cm vacuum ducts

Observing Timeline

Credit: https://observing.docs.ligo.org/plan/

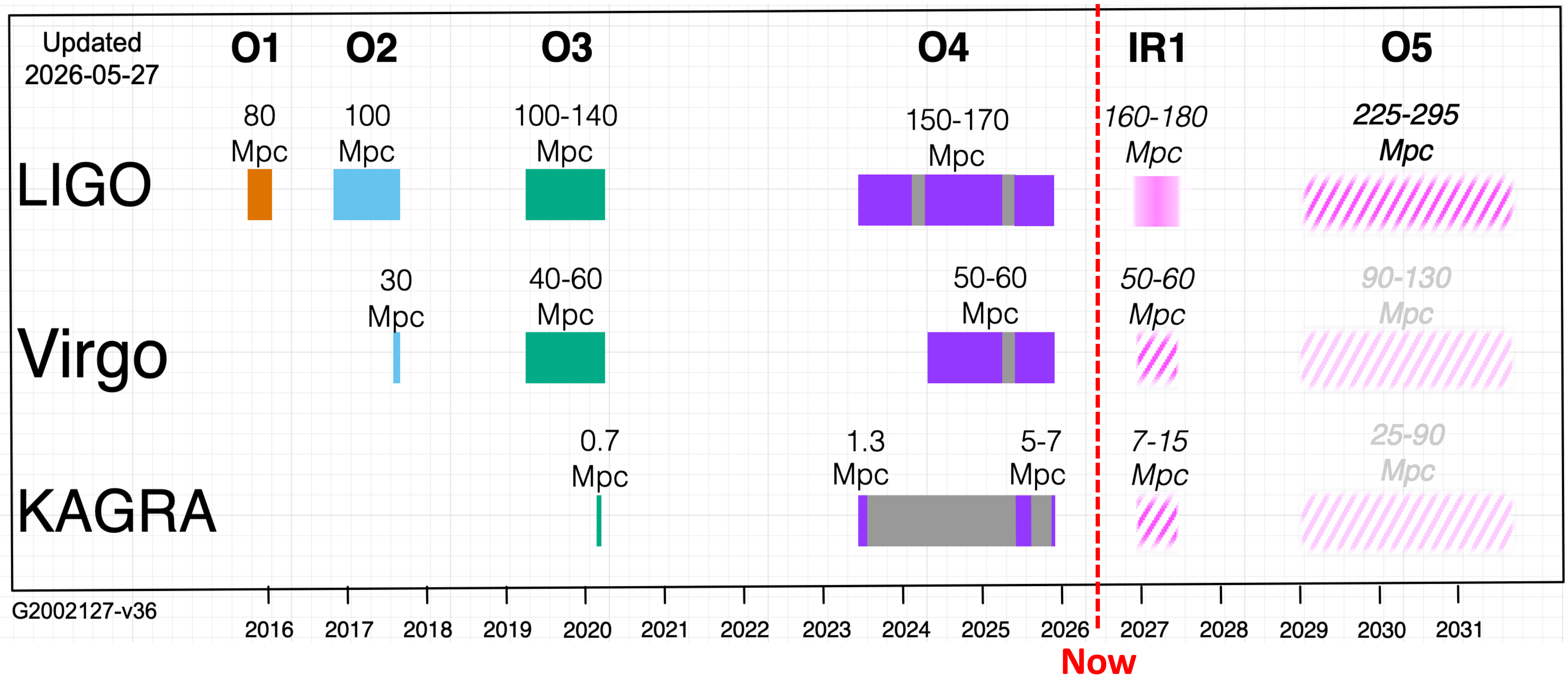

Compact Binary Coalescence (CBC)

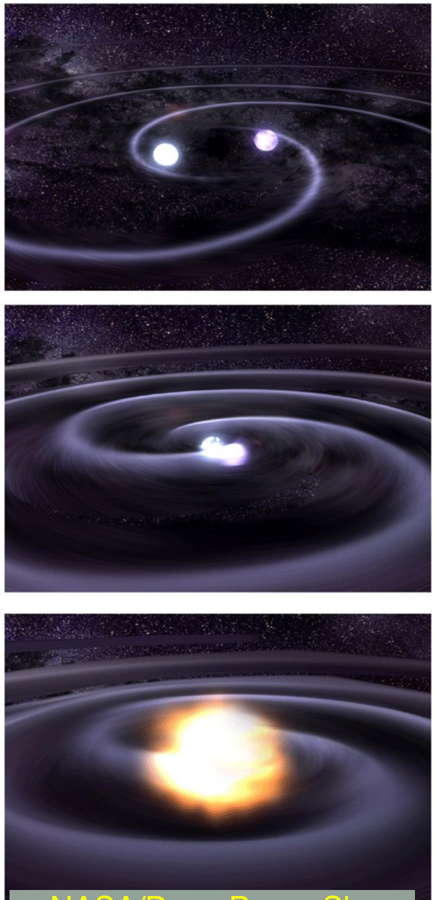

NASA/Dana Berry, Sky Works Digital

- **Primary (and so far only confirmed) source**
- **Three categories:**
  - ➢ Binary Black Hole (BBH)
  - ➢ Neutron Star – Black Hole (NSBH)
  - ➢ Binary Neutron Star (BNS)

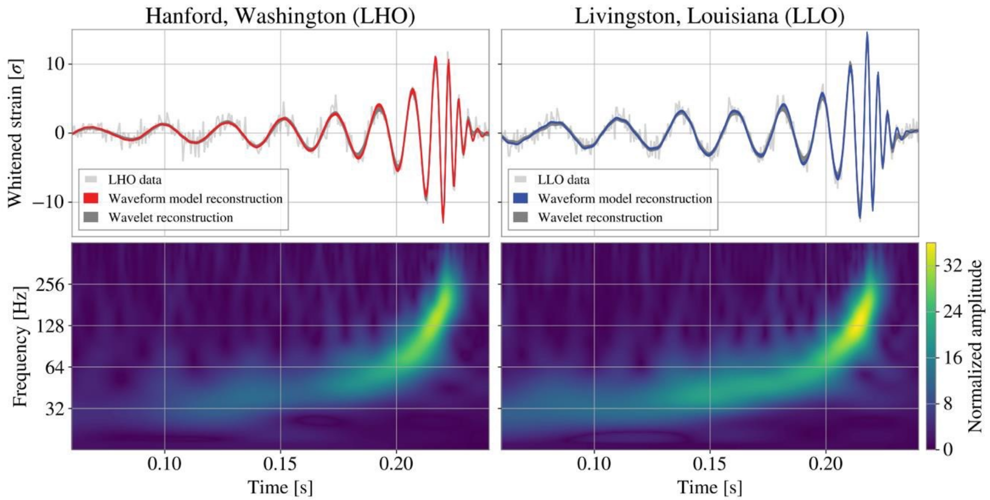

Credit: LIGO-Virgo-KAGRA, PRL **135**, 111403 (2025).

Cumulative GW Detections

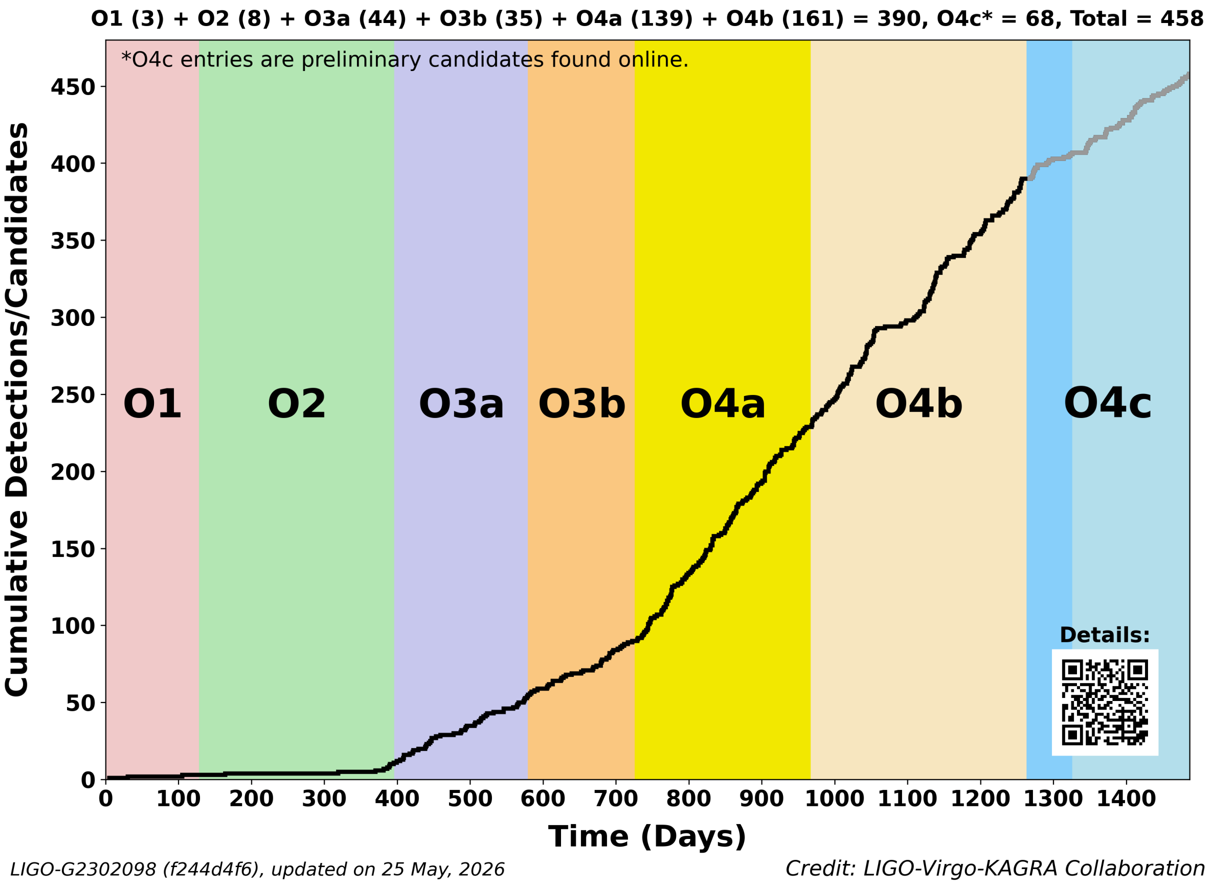

~450 CBCs have been detected!

- 390 events from O1–O4b have been released.

See the latest event catalog:
LVK, arXiv: 2605.27225

Detection rate~1/(a few days)

Observing Timeline

Credit: https://observing.docs.ligo.org/plan/

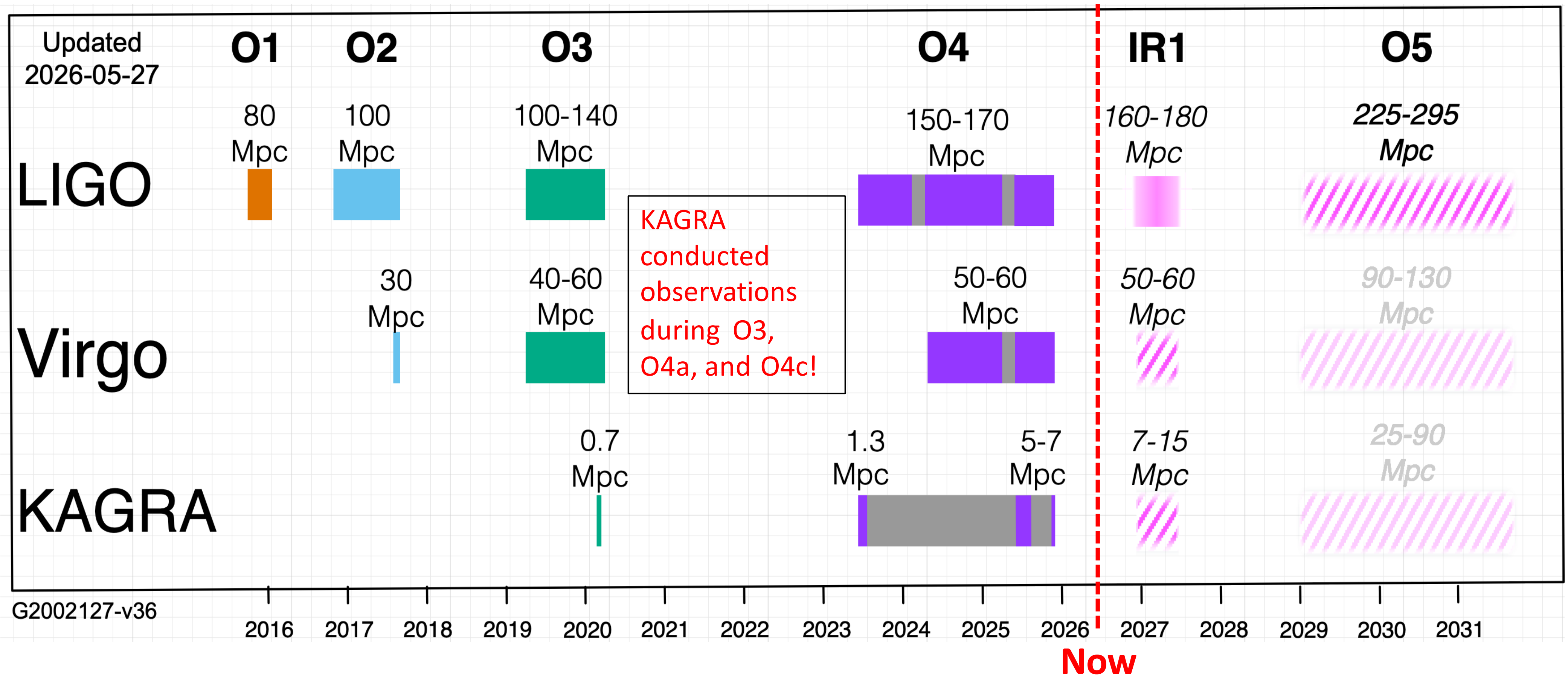

KAGRA Optical Configuration for O4 (PRFPMI)

All mirrors at cryogenic temperature (O4bc)

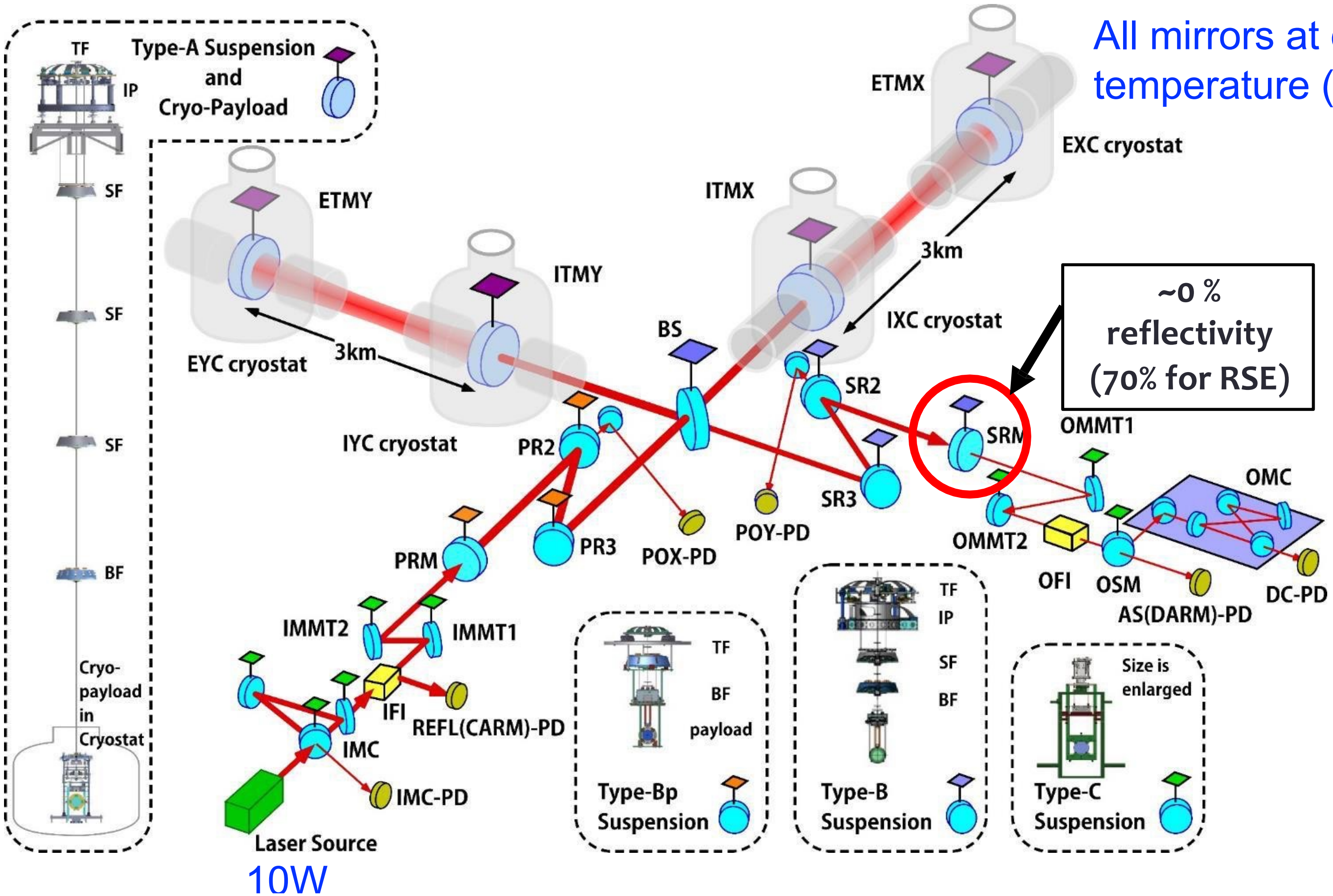

KAGRA O4a

- **Period:**
  24th May 08:00 (JST)–21st June 08:00 (JST) in 2023
- **BNS range:** ~ 1.3 Mpc (~ 0.7 Mpc in O3GK)
- **Duty cycle:** ~ 80% (53.2% in O3GK) including weekly maintenance
- Main lock-loss sources are earthquakes.

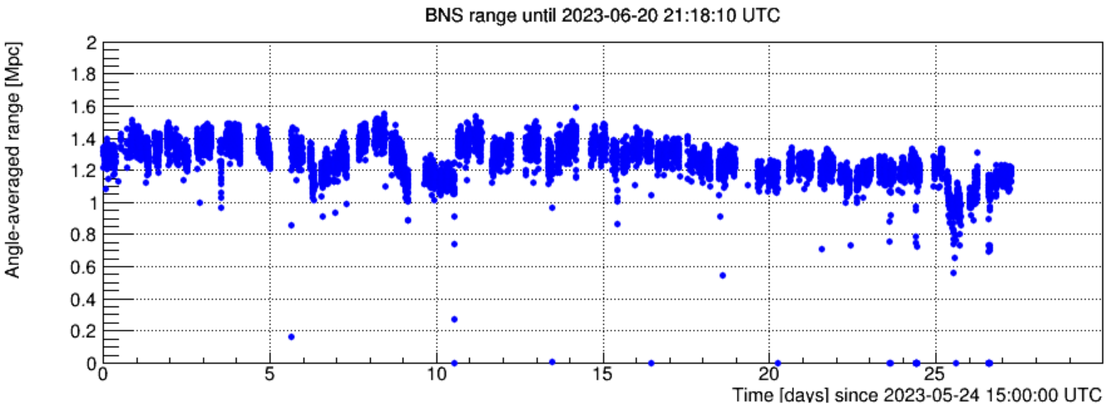

Figure: Binary neutron star (BNS) range of KAGRA during O4a

Observing Timeline

Credit: https://observing.docs.ligo.org/plan/

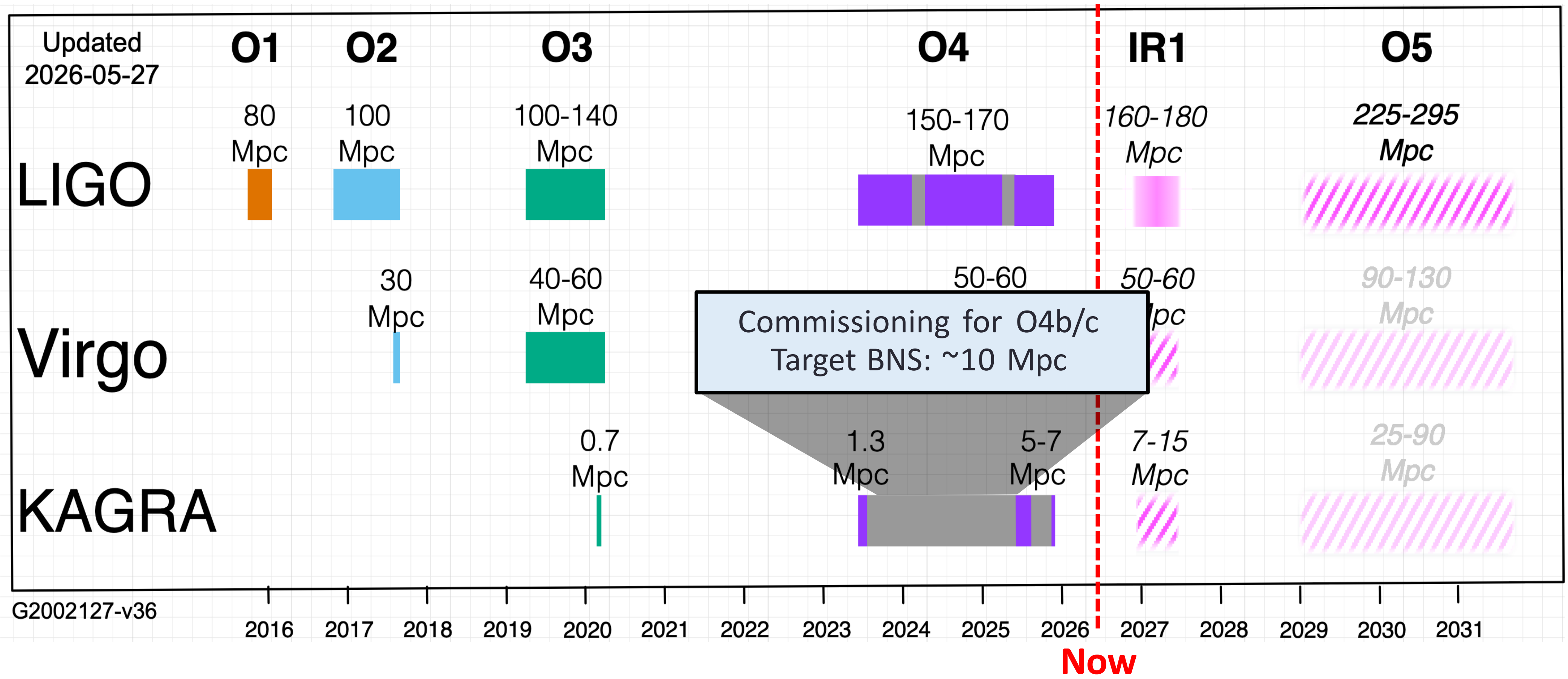

Noto Earthquakes

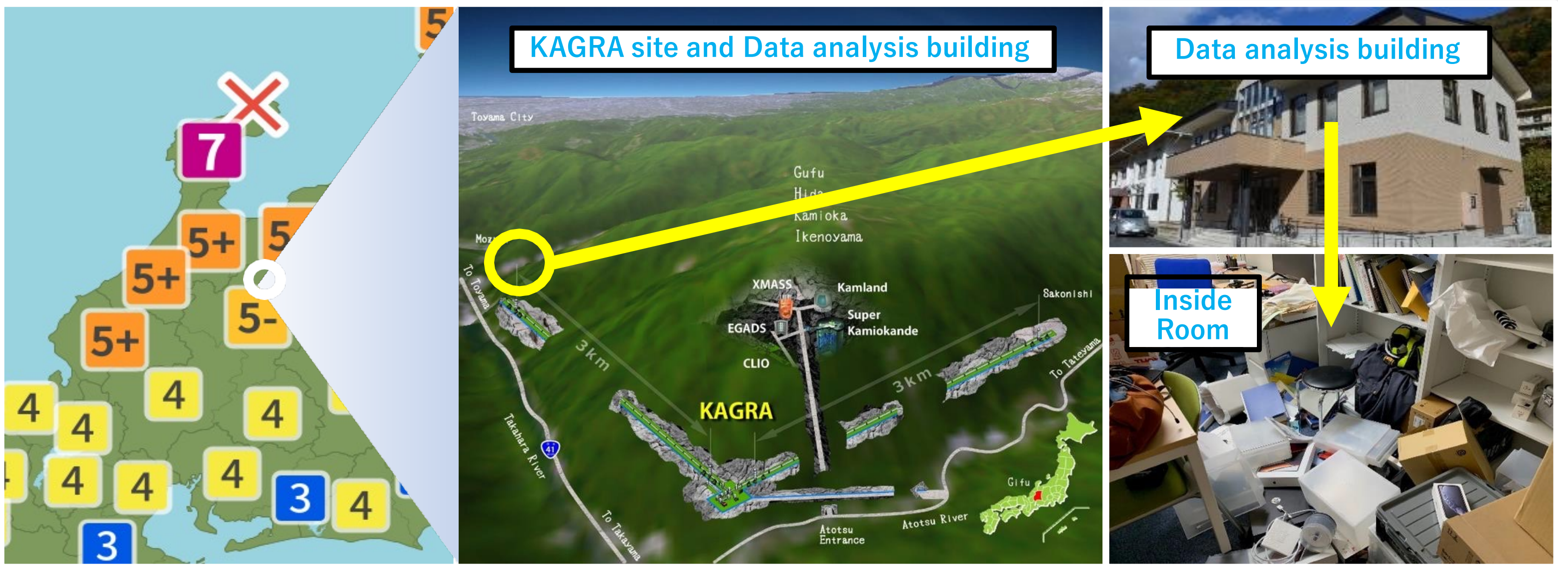

List of Large Earthquakes in the past 100 years

- 1909 Aug 14, M6.8【Anegawa】Lv.3
- 1944 Dec 7, M7.9【Tounankai】Lv.4
- 2011 Feb 17, M5.5【Hida area】Lv.3～4
- 2023 May 5, M6.5【Noto Peninsula】LV.2～3
- 2024 Jan 1, M7.6【Reiwa 6 Noto Peninsula】LV 5- (Red means KAGRA was operated.)

Lv.5- was the largest earthquake at least in the last 100 years

Noto Earthquakes

10 out of 20 mirror suspensions were damaged …

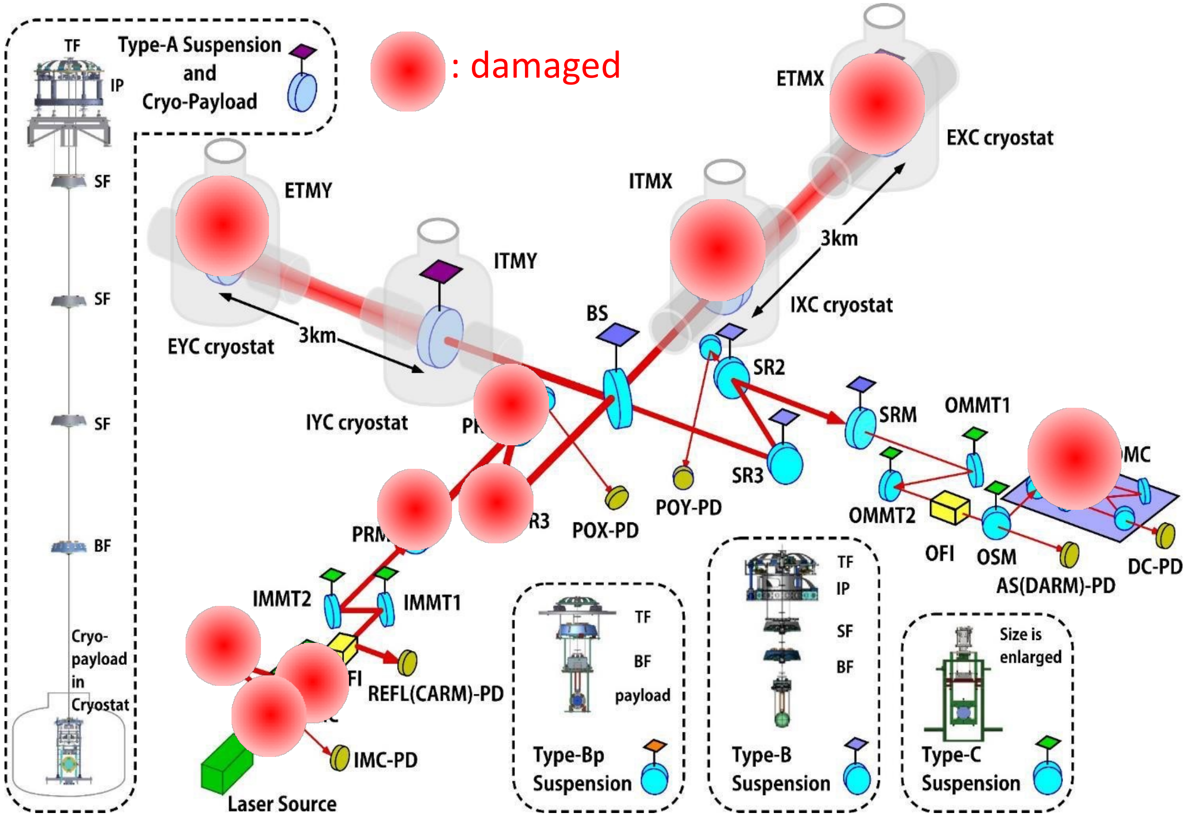

Signal wire cut

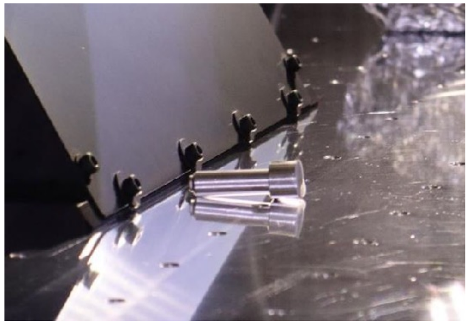

Magnet dropoff

The recovery was completed, and commissioning resumed in July 2024, thanks to the tremendous efforts of the on-site researchers.

Commissioning toward O4c

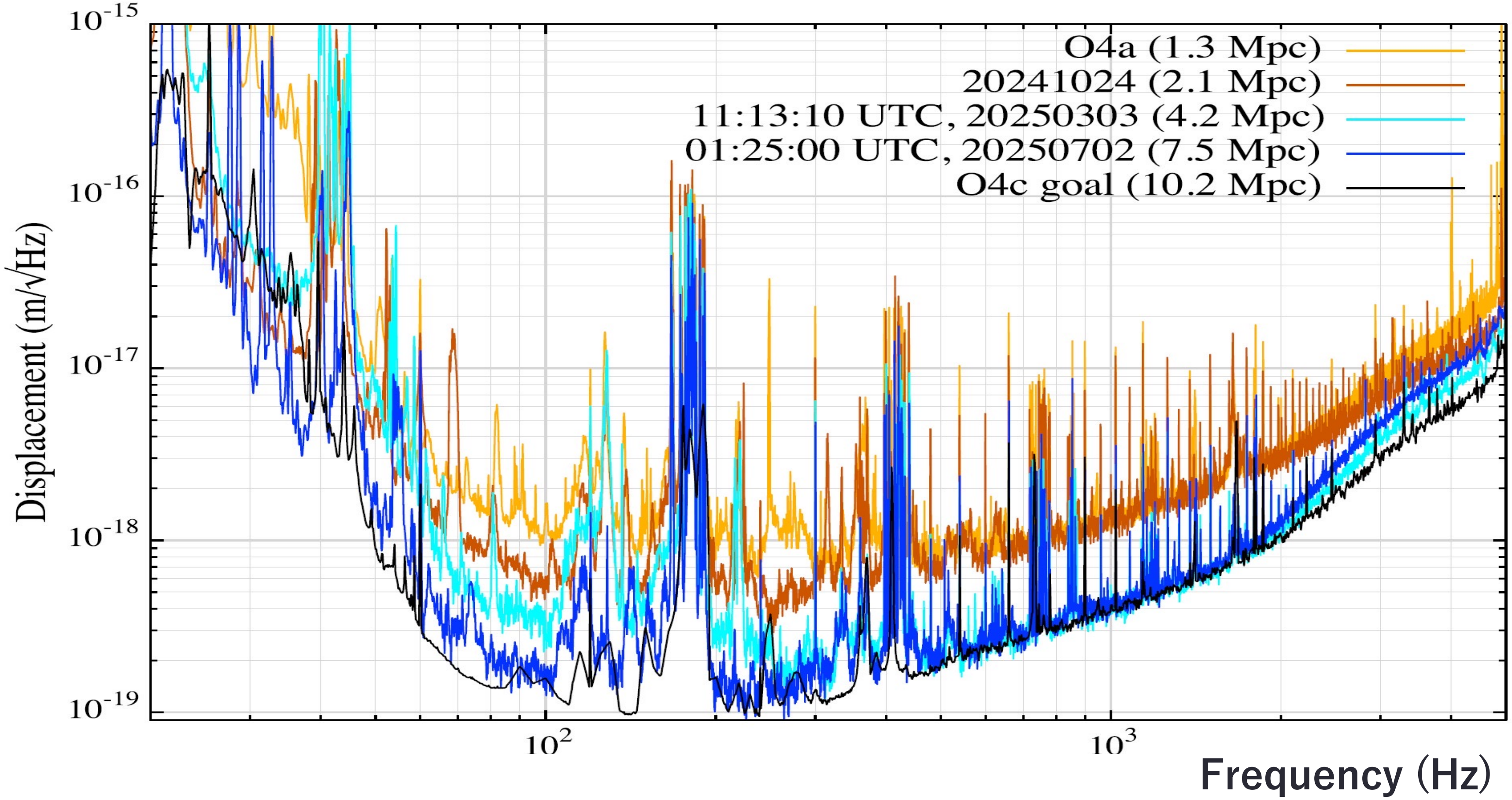

Commissioning toward O4c

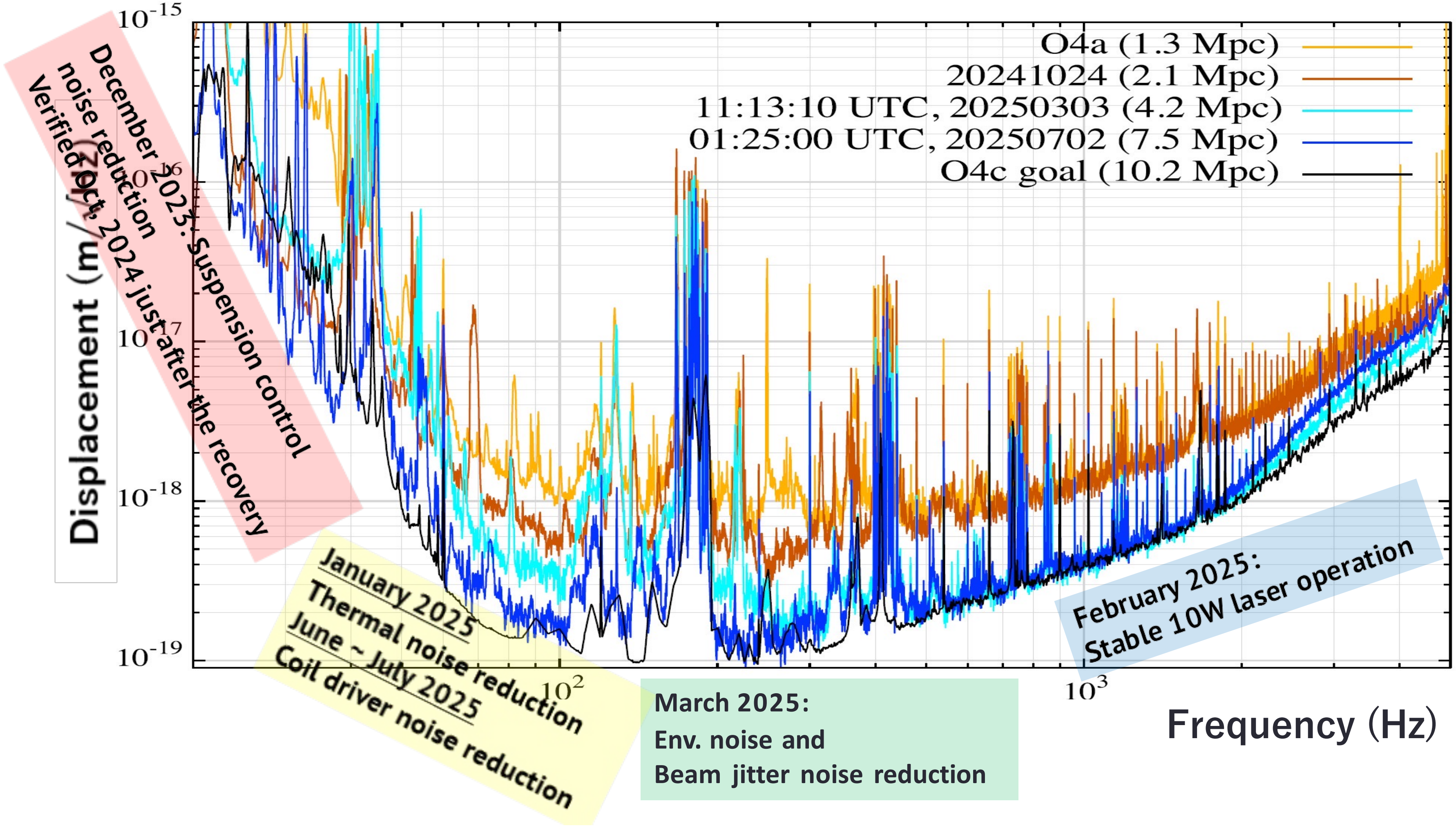

KAGRA O4c

- **Period:** 11th June – 18th November in 2025
- Affected by earthquakes in Tokara Islands (mid July) and Kamchatka Peninsula (July 30–August)
- Failure of main laser (August 15th –)

➔Recovered on November 14th

Gravitational Wave Detector Network

Operational Snapshot as of Jun. 11, 2025 15:16:56 UTC

Detector	Status	Duration [hh:mm]	Latency [s]
GEO600	Observing	00:17	36
LIGO Hanford	Observing	00:19	18
LIGO Livingston	Calib not ready	20:52	62
Virgo	Down	07:43	29
KAGRA	Observing	02:10	37

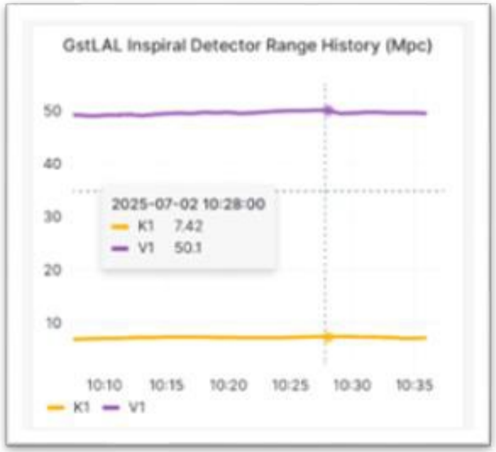

KAGRA's Best BNS Range ~ 7.5 Mpc

Figure: BNS range of KAGRAon July 2, 2025.

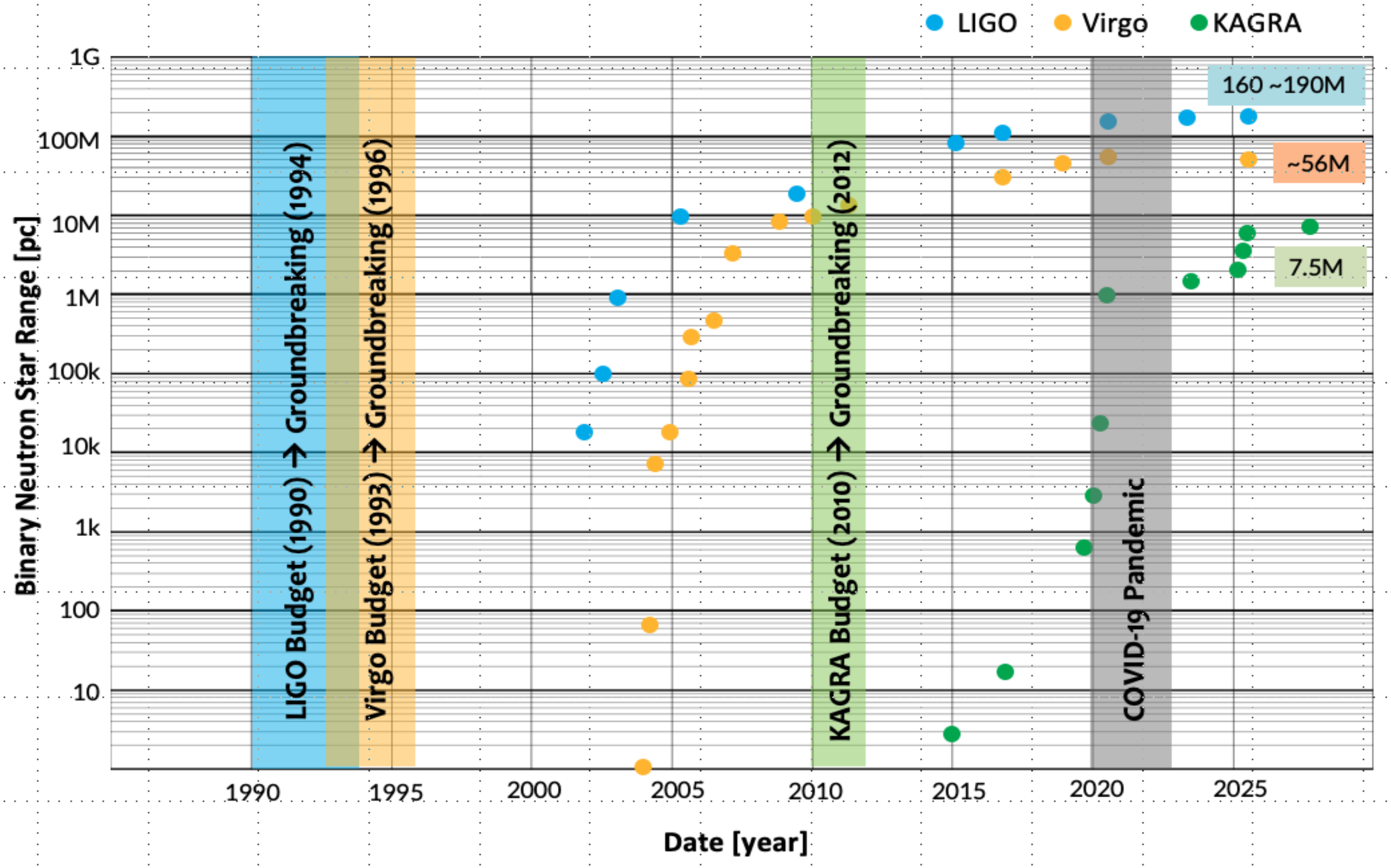
LIGO
Virgo
KAGRA
160 ~190M
~56M
7.5M
1G
100M
10M
1M
100k
10k
1k
100
10
Binary Neutron Star Range [pc]
LIGO Budget (1990) → Groundbreaking (1994)
Virgo Budget (1993) → Groundbreaking (1996)
KAGRA Budget (2010) → Groundbreaking (2012)
COVID-19 Pandemic
1990
1995
2000
2005
2010
2015
2020
2025
Date [year]

Future Observations

Credit: https://observing.docs.ligo.org/plan/

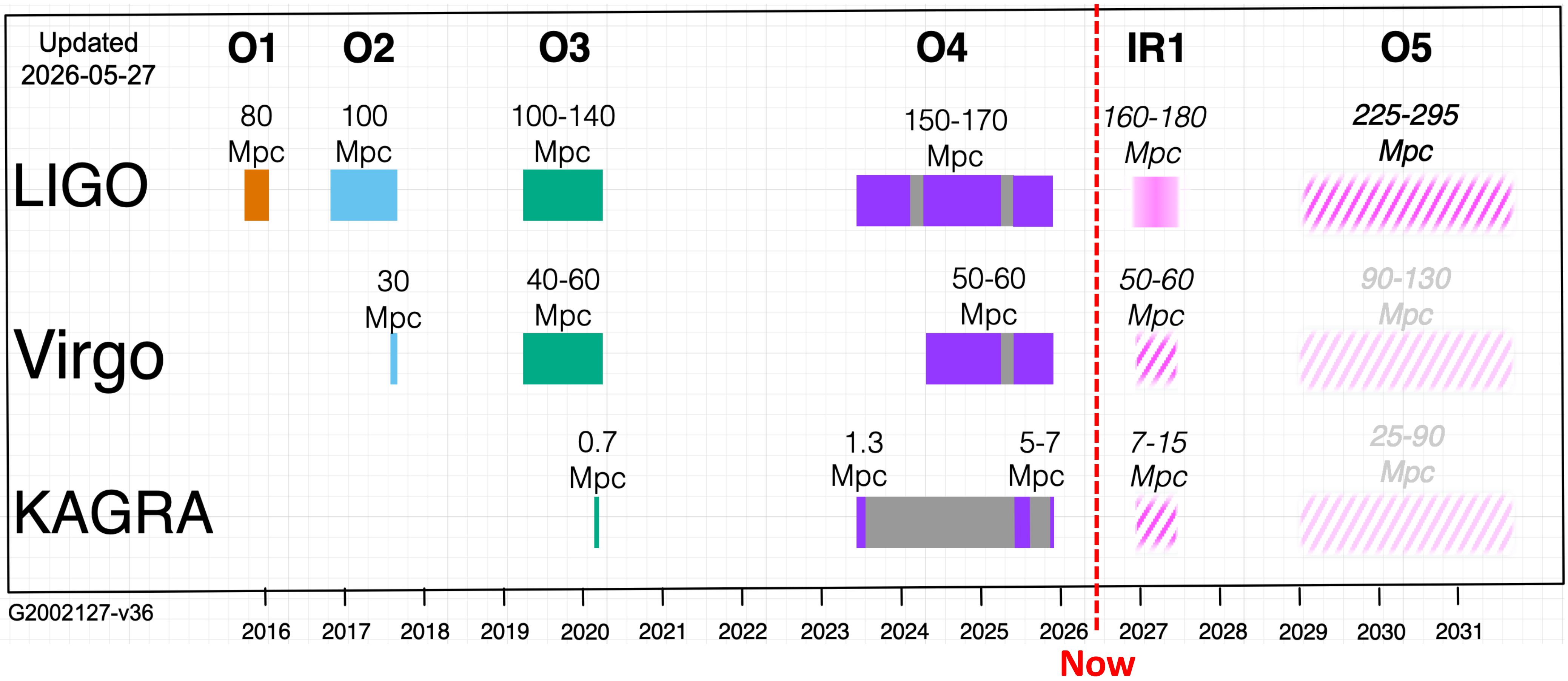

KAGRA beyond O5

KAGRA collaboration, arXiv: 2508.03392

arXiv > gr-qc > arXiv:2508.03392

Search... All fields Search

Help | Advanced Search

General Relativity and Quantum Cosmology

[Submitted on 5 Aug 2025]

Decadal upgrade strategy for KAGRA toward post-O5 gravitational-wave astronomy

KAGRA Collaboration: T. Akutsu, M. Ando, M. Aoumi, A. Araya, Y. Aso, L. Baiotti, R. Bajpai, K. Cannon, A. H.-Y. Chen, D. Chen, H. Chen, A. Chiba, C. Chou, M. Eisenmann, K. Endo, T. Fujimori, S. Garg, D. Haba, S. Haino, R. Harada, H. Hayakawa, K. Hayama, S. Fujii, Y. Himemoto, N. Hirata, C. Hirose, H.-F. Hsieh, H.-Y. Hsieh, C. Hsiung, S.-H. Hsu, K. Ide, R. Iden, S. Ikeda, H. Imafuku, R. Ishikawa, Y. Itoh, M. Iwaya, H-B. Jin, K. Jung, T. Kajita, I. Kaku, M. Kamiizumi, N. Kanda, H. Kato, T. Kato, R. Kawamoto, S. Kim, C.Kim, K. Kobayashi, K. Kohri, K. Kokeyama, K. Komori, A. K. H. Kong, T. Koyama, J. Kume, S. Kuroyanagi, S. Kuwahara, K. Kwak, S. Kwon, H. W. Lee, R. Lee, S. Lee, K. L. Li, L. C.-C. Lin, E.-T.-Lin, Y.-C. Lin, G. C. Liu, K. Maeda, M. Meyer-Conde, Y. Michimura, K. Mitsuhashi, O. Miyakawa, S. Miyoki, S. Morisaki, Y. Moriwaki, M. Murakoshi, K. Nakagaki, K. Nakamura, H. Nakano, T. Narikawa, L. Naticchioni, L. Nguyen Quynh, Y. Nishino, A. Nishizawa, K. Obayashi, M. Ohashi, M. Onishi, K. Oohara, S. Oshino, R. Ozaki, M. A. Page, K.-C. Pan, B.-J. Park, J. Park, F. E. Pena Arellano, N. Ruhama, S. Saha, K. Sakai, Y. Sakai et al. (54 additional authors not shown)

The KAGRA Collaboration has investigated a ten-year upgrade strategy for the KAGRA gravitational wave detector, considering a total of 14 upgrade options that vary in mirror mass, quantum noise reduction techniques, and the quality of cryogenic suspensions. We evaluated the scientific potential of these configurations with a focus on key targets such as parameter estimation of compact binary coalescences, binary neutron star post-merger signals, and continuous gravitational waves. Rather than aiming to improve all science cases uniformly, we prioritized those most sensitive to the detector configuration. Technical feasibility was assessed based on required hardware developments, associated R\&D efforts, cost, and risk. Our study finds that a high-frequency upgrade plan that enhances sensitivity over a broad frequency range above ~200 Hz offers the best balance between scientific return and technical feasibility. Such an upgrade would enable sky localization of binary neutron star mergers at 100 Mpc to better than 0.5 deg^2 in a LIGO-Virgo-KAGRA network, and improve the measurement precision of tidal deformability parameter by approximately 10% at median, compared to a network without KAGRA.

Access Paper:

- View PDF
- HTML (experimental)
- TeX Source

view license

Current browse context:
gr-qc

< prev | next >

new | recent | 2025-08

Change to browse by:

astro-ph

astro-ph.IM

References & Citations

- INSPIRE HEP
- NASA ADS
- Google Scholar
- Semantic Scholar

Export BibTeX Citation

Bookmark

KAGRA beyond O5: Sensitivity Improvements at kHz

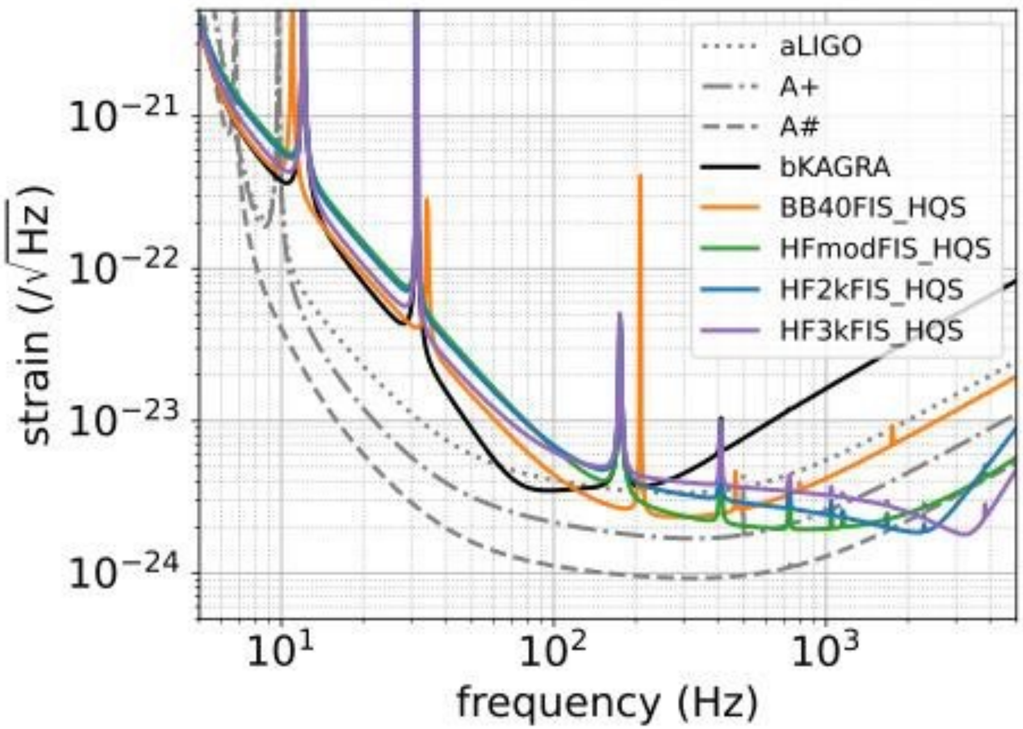

Figure: KAGRA's representative sensitivity options for O6

- **HF** vs **BB**:
  High Frequency vs Broad Band
- **mod/2k/3k**: HF variants optimized for different target frequencies
- **A+** and **A#**: LIGO's design sensitivity for O5 and O6
- **Why HF with KAGRA?**
  - ➢ Sapphire's high thermal conductivity mitigates thermal lensing effects, allowing high laser power

KAGRA beyond O5: Sensitivity Improvements at kHz

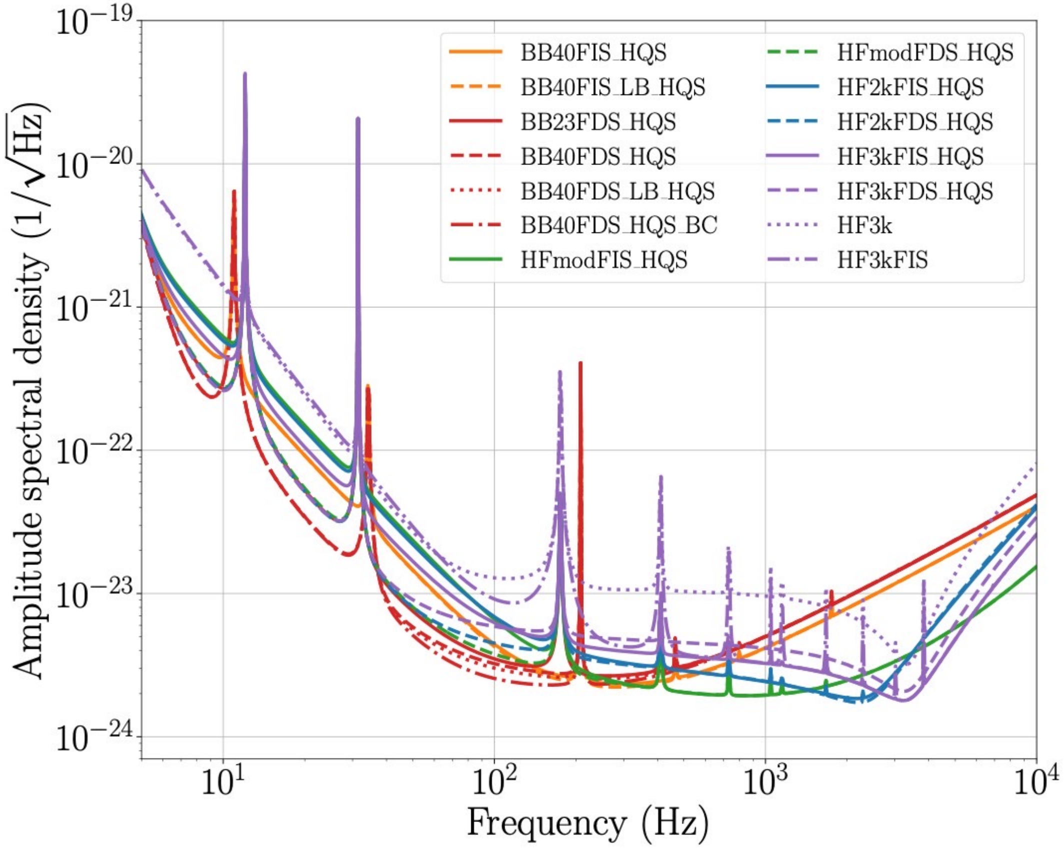

Figure: KAGRA's sensitivity options for O6

We considered 14 configurations.

- **HF** vs **BB**:
  High Frequency vs Broad Band
- **mod/2k/3k**: HF variants optimized for different target frequencies
- **23** vs **40**: Mass of mirror (in kg)
- **FIS** vs **FDS**:
  Frequency-Independent Squeezing vs Frequency-Dependent Squeezing
- **LB: Larger Beam**
- **BC: Better Coating (e.g. AlGaAs)**
- **HQS: High Q Suspensions**

Observable Range and Event Rate

Configuration	BNS Range (Mpc)	Annual Detections		
		BNS	NSBH	BBH
BB40FIS_HQS	144	$4.2^{+4.7}_{-2.5}$	$0.78^{+0.88}_{-0.46}$	48^{+55}_{-28}
BB40FIS_LB_HQS	150	$4.7^{+5.3}_{-2.8}$	$0.88^{+0.99}_{-0.51}$	54^{+61}_{-31}
BB23FDS_HQS	162	$6.0^{+6.7}_{-3.5}$	$1.2^{+1.4}_{-0.7}$	71^{+80}_{-42}
BB40FDS_HQS	184	$8.8^{+9.9}_{-5.1}$	$1.9^{+2.1}_{-1.1}$	100^{+110}_{-60}
BB40FDS_LB_HQS	194	10^{+12}_{-6}	$2.1^{+2.4}_{-1.3}$	120^{+130}_{-70}
BB40FDS_HQS_BC	218	15^{+16}_{-8}	$3.0^{+3.4}_{-1.8}$	150^{+170}_{-90}
HFmodFIS_HQS	124	$2.6^{+3.0}_{-1.5}$	$0.44^{+0.49}_{-0.25}$	25^{+28}_{-14}
HFmodFDS_HQS	166	$6.4^{+7.2}_{-3.8}$	$1.2^{+1.4}_{-0.7}$	66^{+75}_{-39}
HF2kFIS_HQS	103	$1.5^{+1.7}_{-0.9}$	$0.27^{+0.3}_{-0.16}$	16^{+18}_{-9}
HF2kFDS_HQS	142	$4.0^{+4.6}_{-2.4}$	$0.82^{+0.92}_{-0.48}$	46^{+52}_{-27}
HF3kFIS_HQS	99.9	$1.4^{+1.6}_{-0.8}$	$0.26^{+0.3}_{-0.15}$	17^{+19}_{-10}
HF3kFDS_HQS	111	$2.0^{+2.2}_{-1.1}$	$0.42^{+0.47}_{-0.25}$	26^{+29}_{-15}
HF3k	44.9	$0.13^{+0.15}_{-0.08}$	$0.028^{+0.031}_{-0.016}$	$2.0^{+2.3}_{-1.2}$
HF3kFIS	71.0	$0.51^{+0.57}_{-0.3}$	$0.084^{+0.095}_{-0.049}$	$5.2^{+5.9}_{-3.1}$

Table 3 of arXiv: 2508.03392 : BNS sensitive ranges and annual detection rates for various KAGRA configurations

Credit: KAGRA collaboration, arXiv: 2508.03392

- **BB** options generally outperform **HF** options
- 40kg and **FDS** better than 23kg and **FIS** respectively.
- The best option (**BB40FDS_HQS_BC**) gives O(100) BBHs and O(10) BNSs per year

Sky Localization

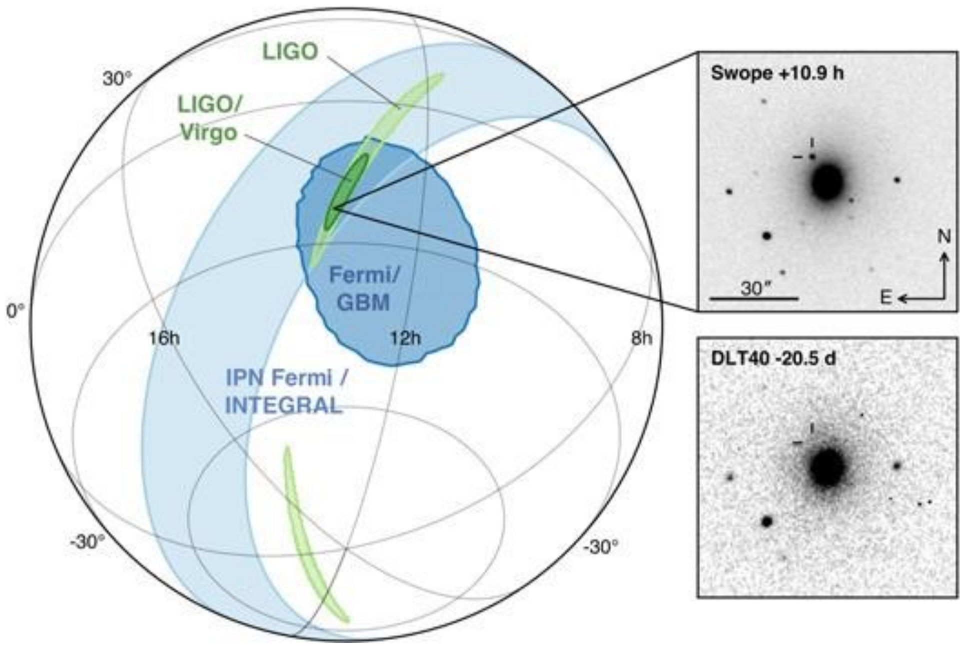

Figure: Sky localization of GW170817

Figure credit: B. P. Abbott et al., ApJL **848**, no.2, L12 (2017).

Localization errors are estimated for 10^5 simulated signals.

- Detector network: 2 LIGO detectors (A# sensitivity), Virgo (O5), and KAGRA
- Two source types:
  $1.4M_{\odot}$- $1.4M_{\odot}$ at 200 Mpc (typical BNSs), $30M_{\odot}$- $30M_{\odot}$ BBHs at 1 Gpc (typical BBHs)
- Localization errors are computed with the Fisher information matrix computed with the IMRPhenomD waveform model

KAGRA beyond O5: Sky Localization

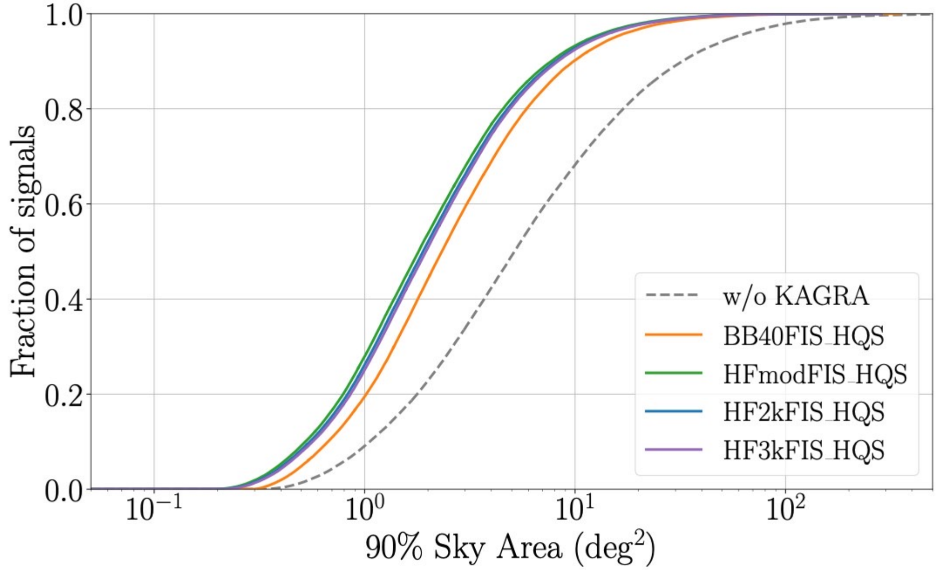

$1.4M_\odot$- $1.4M_\odot$ BNSs at 200Mpc

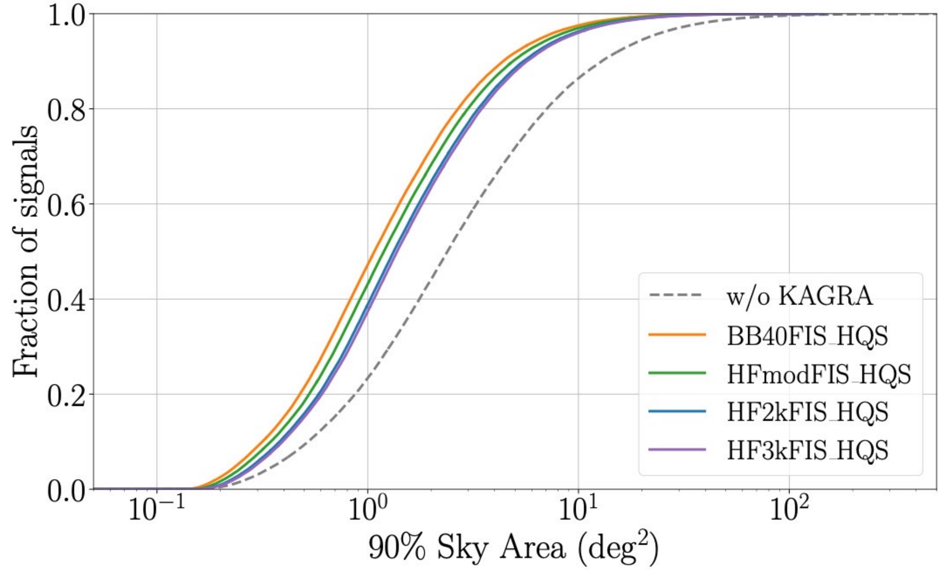

$30M_\odot$- $30M_\odot$ BBHs at 1Gpc

Figure: Cumulative distribution of sky localization errors

Detector network: 2 LIGO detectors (A# sensitivity), Virgo (O5 sensitivity), and KAGRA

HF options perform better (worse) for BNSs (BBHs) than BB options

BNS Post-Merger Signal

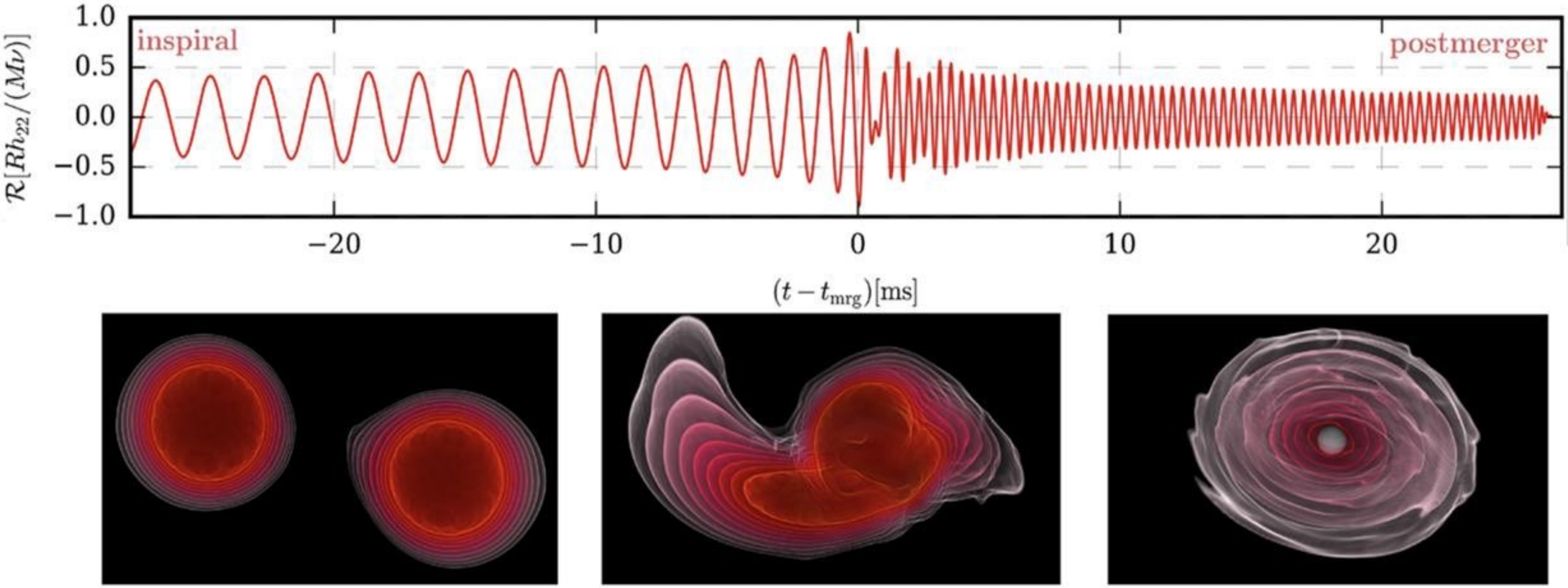

Credit: T. Dietrich, T. Hinderer, and A. Samajdar, Gen. Rel. Grav. **53**, no. 3, 27 (2021).

BNS Post-Merger Signal: Detectability

PSD	Horizon (Mpc)	Detection Rate (1/year)
A#	60.1–90.7	2×10^{-3}-8×10^{-2}
BB40FIS_HQS	16.7–25.1	4×10^{-5}–2×10^{-3}
HFmodFIS_HQS	55.7–84.2	1×10^{-3}–6×10^{-2}
HF2kFIS_HQS	66.9–104.0	2×10^{-3}–1×10^{-1}
HF3kFIS_HQS	67.3–132.4	2×10^{-3}–2×10^{-1}

Table: Horizon distances and detection rates of BNS post-merger signal for various KAGRA configurations

Method

- SNR threshold: 5
- Event rate: $105.5^{+190.2}_{-83.9}\ \mathrm{Gpc^{-3}yr^{-1}}$ (LIGO-Virgo-KAGRA (2021)).
- Computed with several numerical waveforms from K. Kiuchi et al. (2020) and Y. Huang et al. (2022) to take into account uncertainties in EoS and waveform.

The **HF2k** and **HF3k** configurations can maximize the detectability of the BNS post-merger signal.

Motivation of classification of Core-Collapse Supernovae model from the detection candidates

- Machine learning–based classification of core-collapse supernovae (CCSNe) has been widely studied. For example, Ref. [1] employed the short-time Fourier transform (STFT) as a preprocessing step and evaluated classification performance using a convolutional neural network (CNN).

✓ It is known that the Hilbert–Huang transform (HHT) provides more detailed time–frequency information.

➢ In this study, our final goal is that we investigate whether using HHT-based inputs can improve the estimation performance🔥

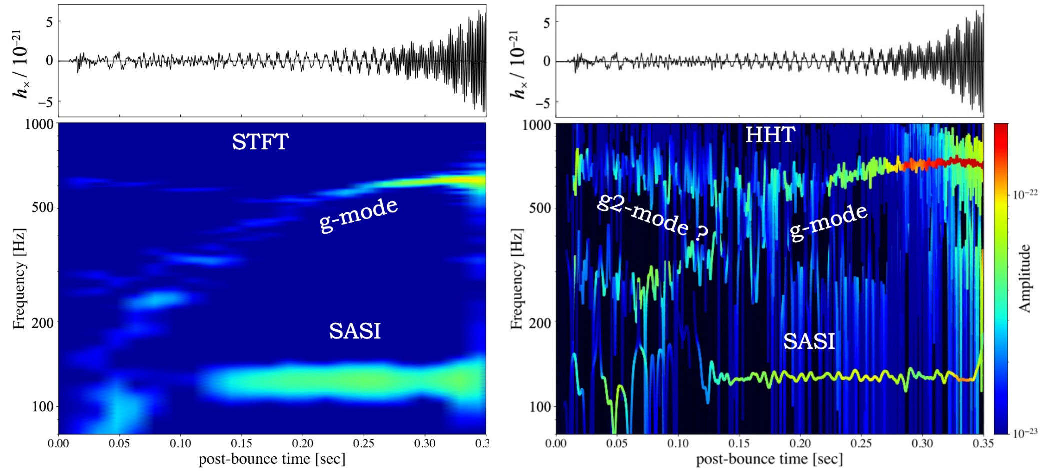

HHT provides higher time–frequency resolution than the short-time Fourier transform (STFT). [2]

[1] Sasaoka, S., Koyama, N., Dominguez, D., Sakai, Y., Somiya, K., Omae, Y., & Takahashi, H. (2023). *Physical Review D*, *108*(12), 123033.
[2] M. Takeda, Y. Hiranuma, et al., Phys. Rev. D104, 084063 (2021)

GWs from 3D CCSNe simulations [1, 2]

The simulation depends on an initial mass, spin, frequency peak, the nuclear equation of states.

There are 46 distinct types of 3D CCSNe at least.

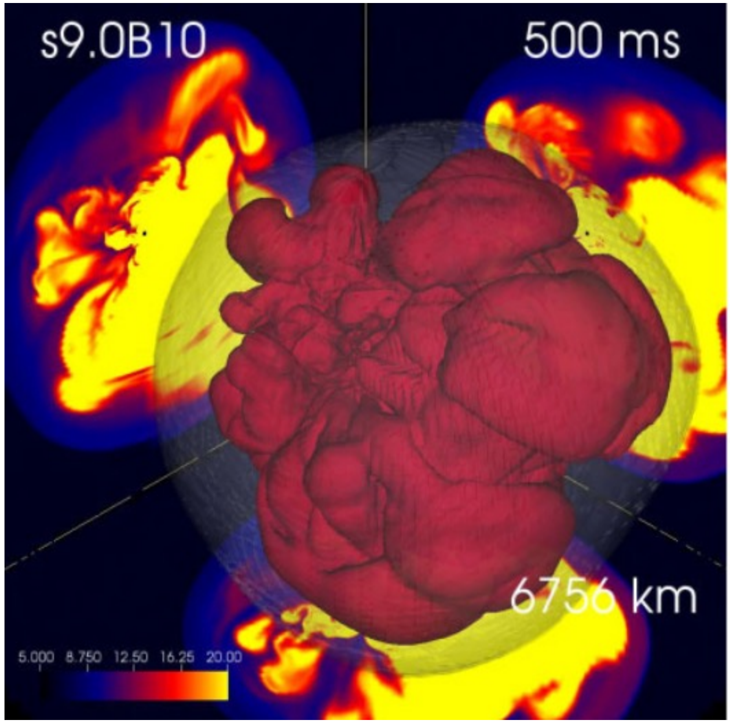

3D simulation of CCSNe[1]

Waveform Family	Numerical Method	GW Features	Waveform Identifier	$M_{\rm star}$ [$M_\odot$]	Ω_c [rad/s]	$f_{\rm peak}$ [Hz]	$E_{\rm GW}$ [$M_\odot c^2$]	Duration [ms]
Abdikamalov *et al.* 2014, 2D [90]	LS220, Shen CoCoNuT	Bounce prompt-conv.	A1O01.0	12	1.0	819	9.4×10^{-9}	50*
			A2O01.0	12	1.0	854	1.7×10^{-8}	50*
			A3O01.0	12	1.0	867	7.0×10^{-9}	50*
			A4O01.0	12	1.0	873	4.2×10^{-9}	50*
Andresen *et al.* 2017, 3D [51]	LS220 CoCoNuT PROMETHEUS	*g*-modes SASI (spiral) convection	s11	11.2	···	642	1.1×10^{-10}	350*
			s20	20	···	687	7.4×10^{-10}	430*
			s20s	20	···	693	1.4×10^{-9}	530*
			s27	27	···	753	4.4×10^{-10}	570*
Andresen *et al.* 2019, 3D [91]	LS220 PROMETHEUS	SASI (spiral) *g*-modes	m15fr	15	0.5	689	2.7×10^{-10}	460*
			m15nr	15	···	820	1.5×10^{-10}	350*
			m15r	15	0.2	801	7.1×10^{-11}	380*
Cerdá-Durán *et al.* 2013, 2D [59]	LS220 CoCoNuT	BH formation *g*-modes, SASI/conv.	Fiducial	35	2.0	922	3.3×10^{-7}	1620
			Slow	35	1.0	987	9.4×10^{-7}	1050
Dimmelmeier *et al.* 2008, 2D [92]	LS, Shen CoCoNuT	Bounce prompt-conv.	s15A2O09-ls	15	4.6	743	2.7×10^{-8}	60*
			s15A3O15-ls	15	13.3	117	5.2×10^{-9}	340*
			s20A3O09-ls	20	9.0	615	2.2×10^{-8}	80*
Kuroda *et al.* 2016, 3D [93]	SFHx, DD2, TM1 3D-GR	*g*-modes SASI	SFHx	15	···	718	2.1×10^{-9}	350*
			TM1	15	···	714	1.7×10^{-9}	350*
Kuroda *et al.* 2017, 3D [94]	SFHx, DD2, TM1 3D-GR	*g*-modes SASI/ convection	s11.2	11.2	···	195	1.3×10^{-10}	190*
			s15.0	15	···	430	3.1×10^{-9}	210*
Mezzacappa *et al.* 2020, 3D [73]	LS220 CHIMERA	*g*-, *p*-modes SASI/ convection	c15-3D	15	···	1064	6.4×10^{-9}	420*
Morozova *et al.* 2018, 2D [95]	LS220, DD2, SFHo FORNAX	*f*-, *g*-, *p*-modes SASI/ convection	M10_LS220	10	···	1594	2.4×10^{-9}	1210
			M10_DD2	10	···	1544	1.7×10^{-9}	1700
			M13_SFHo	13	···	976	1.1×10^{-8}	1360
			M19_SFHo	19	···	1851	6.3×10^{-8}	1540
Müller *et al.* 2012, 3D [71]	JM PROMETHEUS	SASI/convection	L15-3	15	···	144	2.2×10^{-11}	1400
			N20-2	20	···	147	1.1×10^{-11}	1500
			W15-4	15	···	208	2.5×10^{-11}	1300

(Table continued)

[1] Nakamura, K., Takiwaki, T., Matsumoto, J., & Kotake, K. (2025). Monthly Notices of the Royal Astronomical Society, 536(1), 280-294.
[2] Szczepańczyk, Marek J., et al. *Physical Review D* 104.10 (2021): 102002.

Samples of the waveforms from 3D-CCSNe simulations

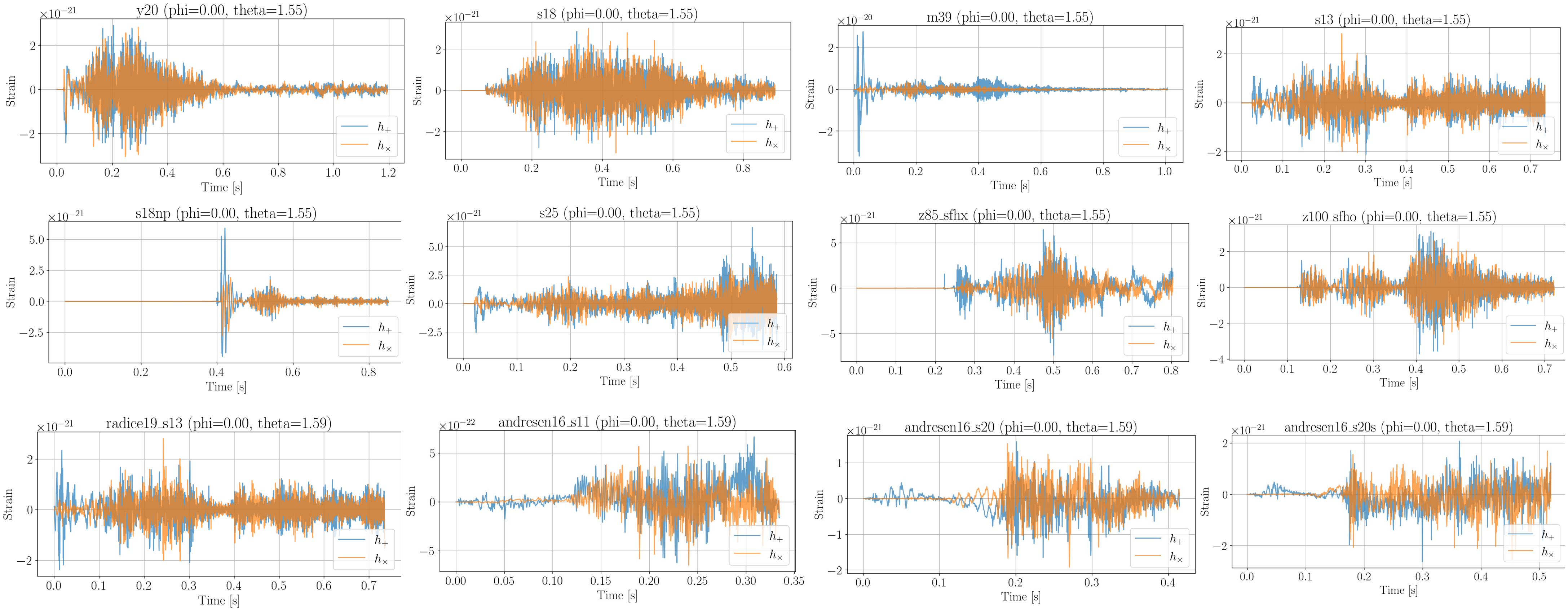

A total of 46 types of 3D-CCSNe waveforms

Einstein Telescope

Next-generation underground observatory designed to detect gravitational waves.
We use a triangle design with 3-detector configuration.

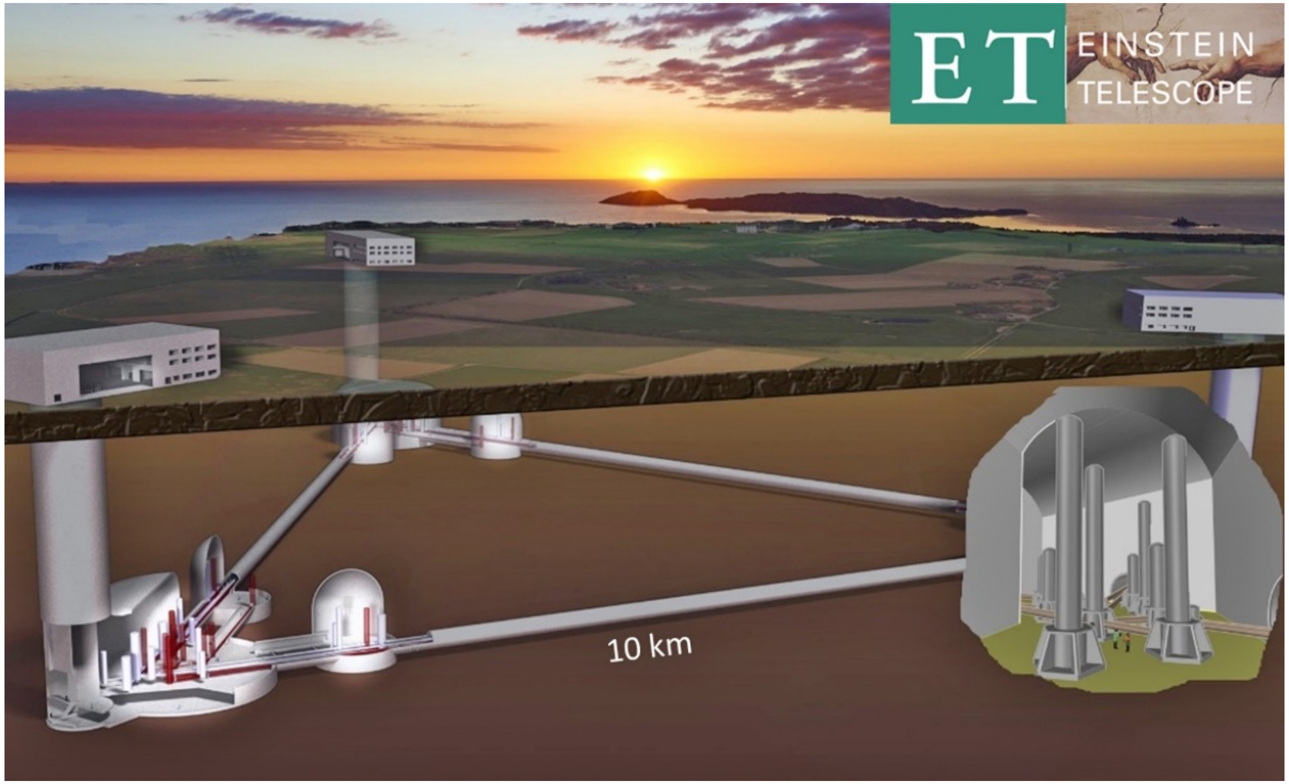

ET will be built in Europe.
The construction is planned to start 2028.

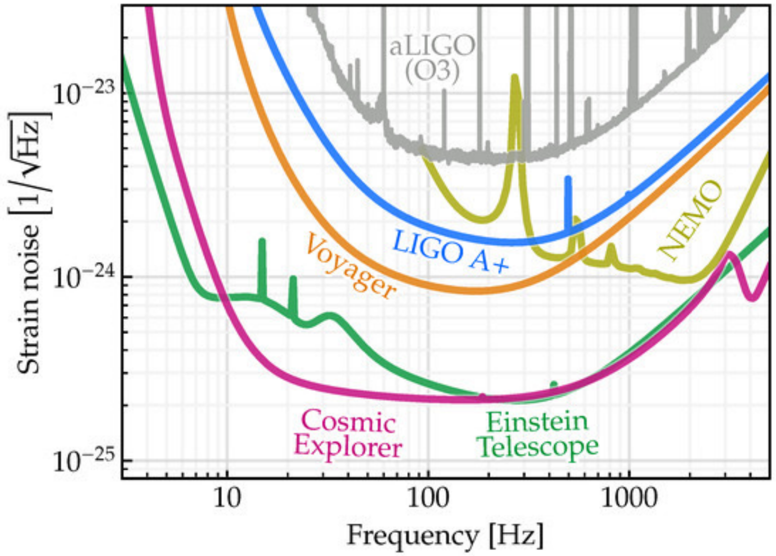

Abac, Adrian, et al. "The science of the Einstein telescope." (2025). arXiv:2503.12263 [gr-qc]

Overview of Our Data Configuration

In CCSNe, asymmetric convection (and instability) within the star is the key to inducing the explosion.

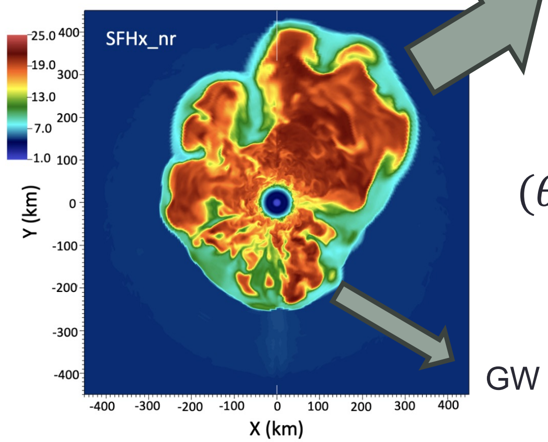

(θ, ϕ)

CCNSe simulation[1]

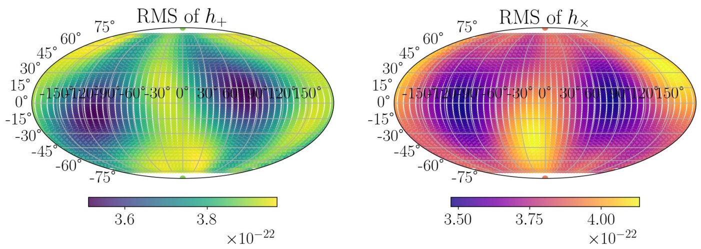

46 types of CCSNe

[Task] Can we classify them?

Attena pattern of a GW detector

$$h(t) = F_+(\text{ra}, \text{dec}, \text{pol}, t)\ h_+(t; \theta, \phi) + F_\times(\text{ra}, \text{dec}, \text{pol}, t)\ h_\times(t; \theta, \phi)$$

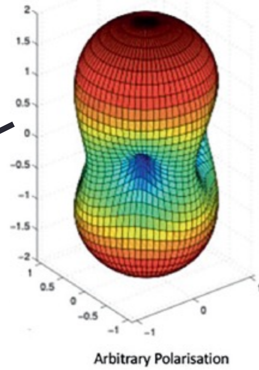

We randomized

$(\theta, \phi, \text{ra}, \text{dec}, \text{pol.})$

~ 531,613 samples totaly

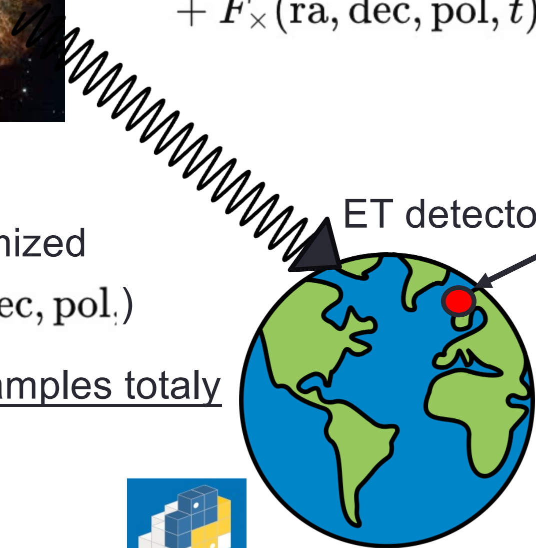

ET detectors[2]

(ra, dec, pol)

PycWB

Source Distance range: 1kpc-100kpc

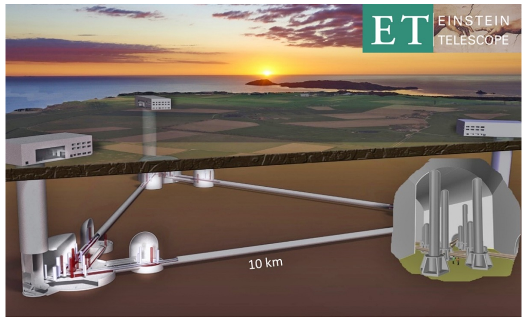

[1] Powell, J., & Müller, B. (2024). *Monthly Notices of the Royal Astronomical Society*, *532*(4), 4326-4339.
[2] Abac, Adrian, et al. "The science of the Einstein telescope." (2025). arXiv:2503.12263 [gr-qc]

Workflow in the this presentation

(1) Time-Series (applied cWB reconstruction)

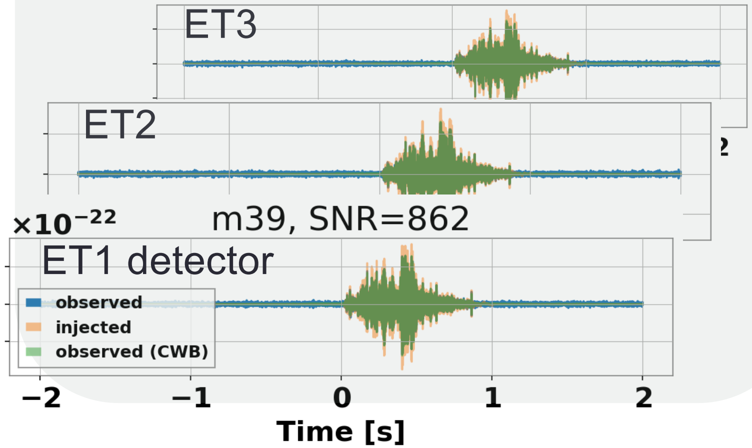

(2) Time-Frequency Representation

Short Time Fourier Transform
In future, we will use HHT

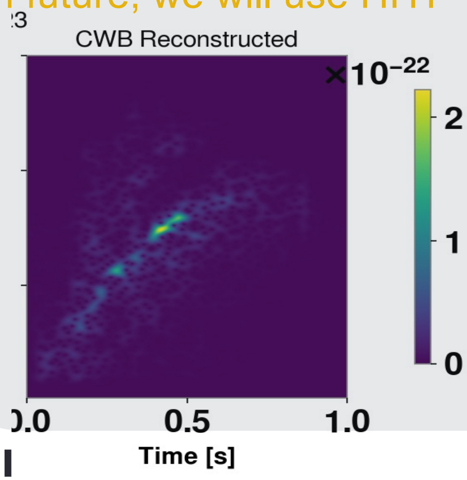

(3) Classfication using Deep Learning

ConvNeXt V2 Block

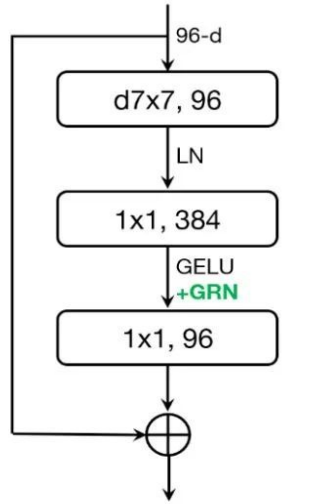

Coherent WaveBusrt[1,2,3]
with O3 configuration

Optional : Data visualization by
Uniform Manifold Approximation and Projection (UMAP) [1]

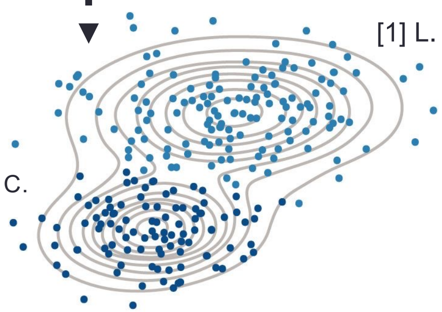

[1] L. McInnes, J. Healy, & J. Melville, arXiv preprint arXiv:1802.03426, (2018).

[1] S. Klimenko, I. Yakushin, A. Mercer, and G. Mitsel-makher, Classical Quantum Gravity 25, 114029 (2008).
[2] S. Klimenko, G. Vedovato, M. Drago, F. Salemi, V. Ti-wari, G. A. Prodi, C. Lazzaro, K. Ackley, S. Tiwari, C. F. Da Silva, and G., Phys. Rev. D 93, 042004 (2016)
[3] M. Drago et al., Coherent WaveBurst, SoftwareX 14, 100678 (2021)

Curriculum Learning

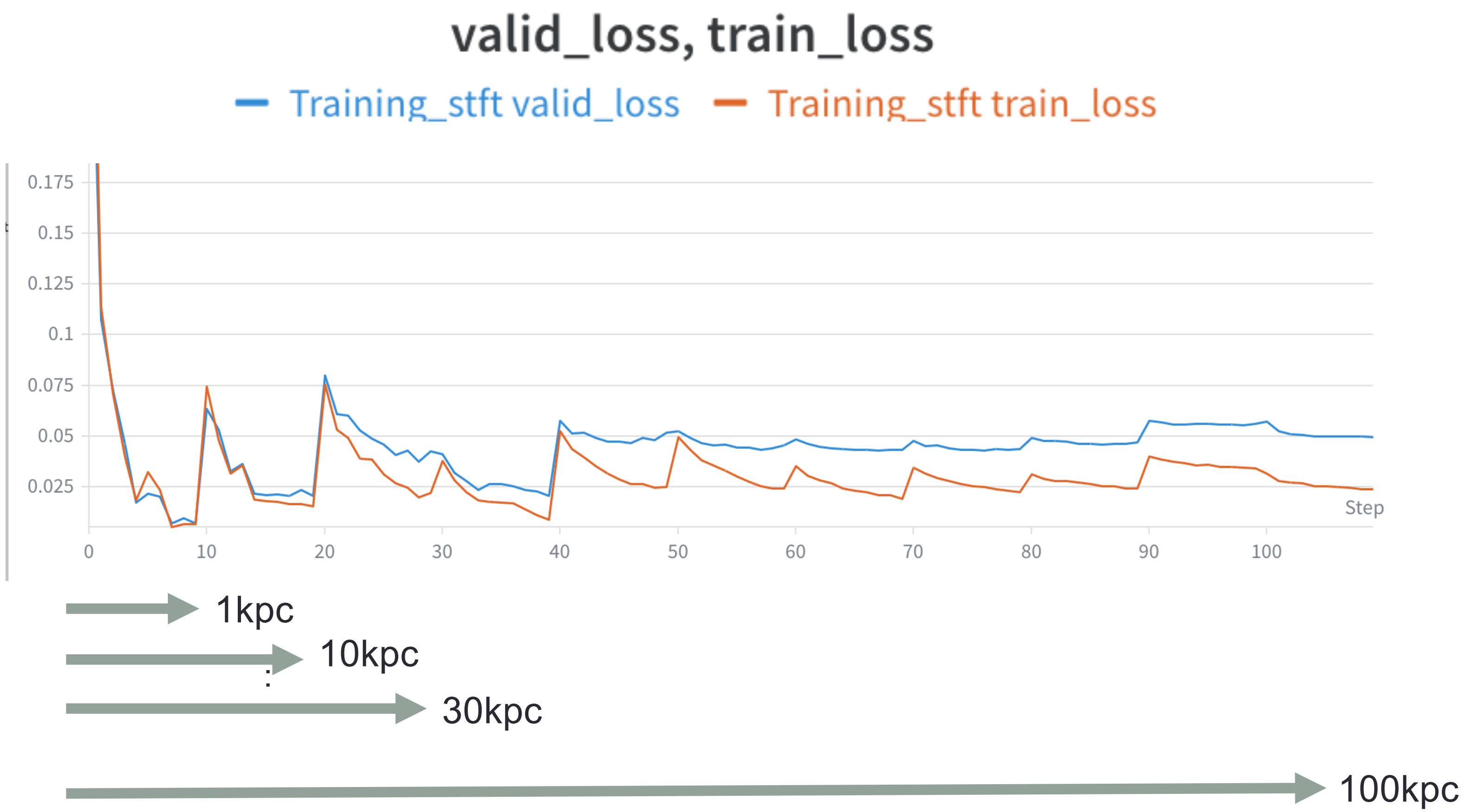

Increase the source distance as the number of epochs increases.

Very Preliminary Results

- Classification Accuracy
  1kpc: 100% (46/46 waveforms)
  10kpc: 99.56% (46/46 waveforms)
  20 kpc: 98.62% (42/46 waveforms)
  30 kcp: 98.95% (40/46 waveforms) distance ~ our galaxy
  40 kpc: 97.01% (35/46 waveforms)
  …
  100 kpc: 98.81% (24/46 waveforms)

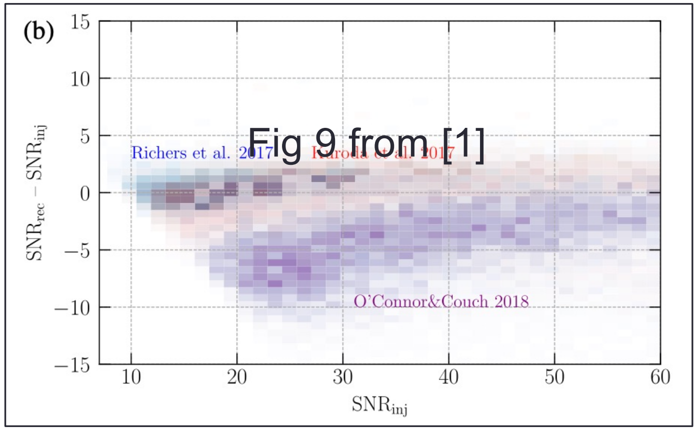

[1] Szczepańczyk, Marek J., et al. *Physical Review D* 104.10 (2021): 102002.

- CCSNe are readily identifiable if they occur in our Galaxy.
- As the source distance increases, cWB reconstruction becomes less reliable, depending on the SN's angle, detector antenna pattern, and waveform duration [1].
- **Future work**: Investigate whether using HHT instead of STFT improves the results or not.
  Investigate whether CCSNe classification is possible without applying cWB reconstruction.

- We are developing a method of universal-Relation Identification with machine learning.

Summary

- KAGRA is an interferometric GW detector located in Japan
  - Built underground to reduce seismic noise
  - Uses cryogenic mirrors and suspensions to reduce thermal noise

- KAGRA participated in O3, O4a, and O4c
  - Achieved a best BNS range ~7.5 Mpc during O4c
  - Suffered damage from the Noto earthquakes but has recovered

- Future plans for KAGRA are under discussion
  - The target BNS range for O5 is > 25 Mpc to enable the first KAGRA GW detection
  - Long-term plans beyond O5 are being explored, including sensitivity improvements around kHz